



Transient mantle cooling linked to regional volcanic shut-down and early rifting in the North Atlantic Igneous Province

J. M. Millett^{1,2} · M. J. Hole² · D. W. Jolley² · S. R. Passey³ · L. Rossetti⁴

Received: 15 May 2020 / Accepted: 15 July 2020
© The Author(s) 2020

Abstract

The Paleocene to Early Eocene Faroe Islands Basalt Group (FIBG) comprises a c. 6.5-km-thick lava flow-dominated sequence located within the centre of the North Atlantic Igneous Province (NAIP). The currently defined pre-breakup and syn-breakup sequences of the FIBG are separated by a significant volcanic hiatus, during which time the coal-bearing Prestfjall Formation was deposited. This major volcanic hiatus is identified across large parts of the NAIP and was preceded on the Faroe Islands by a reduction in eruption rate evidenced by an increased number and thickness of inter-lava sedimentary beds between the simple lava flows of the pre-breakup Beinisvørd Formation. High tempo eruptions resumed after this hiatus with the development of the compound lava flow fields of the Malinstindur Formation which reveal limited evidence for inter-lava breaks. In order to investigate this key transition, flow by flow geochemical sampling of a composite c. 1.1-km-thick lava flow sequence spanning this transition were collected and analysed. Three chemically distinct groups are defined based on rare earth elements (REEs) and incompatible trace element signatures. Two high-Ti groups ($\text{TiO}_2 > 2 \text{ wt}\%$), B2 and B3, dominate the sampled Beinisvørd Formation and display light REE-enriched signatures (La/Yb_N c. 2.9–5.9) and evidence for garnet in the source melting region (Dy/Yb_N c. 1.5–1.6). At the very top of the Beinisvørd Formation, a distinct group of lava flows, B1, displaying lower TiO_2 for a given MgO wt% (TiO_2 c. 1–2 wt%), weakly light REE-enriched profiles (La/Yb_N c. 1.7–2.4) and a spinel-dominated mantle melting signature (Dy/Yb_N c. 1.1–1.2) is identified. Sr, Nd and Pb isotopic signatures for the three groups overlap, revealing limited evidence of crustal contamination, and therefore supporting a mantle melting origin for inter-group variations, rather than source composition or contamination. The group B1 lava flows form a unique stratigraphic occurrence on the islands and provide clear evidence for both a reduction in the initial pressure of melting, alongside an increase in the overall degree of partial melting relative to groups B2 and B3. Increased partial melting is interpreted as evidence for the early onset of rifting and lithospheric thinning to the north of the Faroe Islands. The accompanying reduction in initial pressure of melting provides the first petrological evidence that a transient reduction in mantle temperature leads to the province-wide volcanic hiatus. Our study demonstrates an intimate linkage between rifting history and fluctuations in mantle temperature highlighting that any over-arching model for the evolution of the NAIP must take both into equal account.

Keywords Faroe Islands Basalt Group · NAIP · Mantle temperature · Transient mantle cooling · Lava flow field correlation

Editorial responsibility: N. Métrich

Electronic supplementary material The online version of this article (<https://doi.org/10.1007/s00445-020-01401-8>) contains supplementary material, which is available to authorized users.

✉ J. M. Millett
john.millett@vbpr.no

¹ VBPR AS, Oslo, Norway

² Department of Geology and Geophysics, University of Aberdeen, Aberdeen, UK

³ CASP, West Building, Madingley Rise, Madingley Road, Cambridge, UK

⁴ Universidade Federal de Mato Grosso, Cuiabá, Mato Grosso, Brazil

Introduction

The North Atlantic Igneous Province (NAIP) comprises one of the largest and best studied large igneous provinces (LIP's) associated with continental breakup (Saunders et al. 1997; Gernigon et al. 2019; Peace et al. 2019; Svensen et al. 2019). However, the linkages between magmatism and rifting in association with continental breakup during the Late Paleocene to Early Eocene remain a topic of intensive study. Most petrological studies find evidence for elevated mantle temperatures during NAIP volcanism albeit with differing excess temperature estimates depending on the method/model (Søager and Holm 2011; Hole et al. 2015; Hole and Natland

2019). However, beyond petrological evidence for elevated temperatures, the causes of excess temperature remain highly contested with some authors preferring a mantle plume (bottom up) origin (e.g. Morgan 1971; Søger and Holm 2011; Koptev et al. 2017; Torsvik et al. 2015; Steinberger et al. 2019), whereas other authors prefer alternative plate tectonic (top-down)-associated origins such as thermal incubation or rifting-induced delamination (Anderson 2013; Petersen et al. 2018; Foulger et al. 2019; Clarke and Beutel 2019). Ignoring the more contentious origin depth for mantle upwelling in the NAIP, several observations associated with volcanism in the NAIP have been clearly presented and serve to illuminate the context of our present study including the following:

1. Volcanic eruptions were not uniformly distributed in space (Saunders et al. 1997; Larsen et al. 1999; Millett et al. 2017) or time, both at the province-wide (Storey et al. 2007; Wilkinson et al. 2017) and more local lava flow sequence scales (Jolley et al. 2012; Larsen et al. 2014).
2. Sedimentary records in basins within and surrounding the NAIP underwent multiple rapid uplift and subsidence events coincident with the main phase of volcanism (Shaw-Champion et al. 2008; Hartley et al. 2011; Stoker et al. 2018).
3. Geophysical evidence from the NAIP oceanic ridge system suggests magmatism has fluctuated or pulsed since breakup (Parnell-Turner et al. 2014).
4. Evidence for magmatism and melting clearly changed with time in response to rifting and changing lithospheric thickness during the syn-breakup phase (Larsen et al. 1999; Millett et al. 2016, Millett et al. 2017; Gernigon et al. 2019)
5. The volcanological facies development of the NAIP changed dramatically during the build-up of major lava piles such as the Faroe Islands Basalt Group (FIBG, Passey and Jolley 2008) and East Greenland (Larsen et al. 1989).

It is therefore well established that major fluctuations in magmatism occurred during the evolution of the NAIP; however, the magmatic nature and origins for these fluctuations, especially during the main phase volcanism spanning the Paleocene to Eocene boundary, remain hotly debated.

In order to investigate the nature of magmatic pulsing in the NAIP, this study focuses on the lava flow sequences of the Faroe Islands Basalt Group. The FIBG comprises an extrusive lava flow-dominated sequence with a cumulative thickness of over c. 6.5 km (Larsen et al. 1999; Jolley and Bell 2002; Passey and Jolley 2008, Fig. 1) located in the centre of the NAIP. The proximity of the Faroe Islands to the eventual site of rifting between Greenland and Europe along with accessible stratigraphy makes it an ideal location to investigate the temporal evolution of

magmatism during continental breakup (Passey and Jolley 2008; Søger and Holm 2009; Millett et al. 2017).

Previous studies have correlated the lava flow geochemical stratigraphy of the FIBG to the onshore lava flow sequence exposed in central East Greenland (Larsen et al. 1999; Søger and Holm 2009; Millett et al. 2017), with the lowermost Lopra and Beinivørð formations generally regarded as pre-breakup, whereas the main upper Malinstindur and Enni formations comprise the syn-breakup sequence (Fig. 1). Evidence for variations in mantle temperature within the FIBG and East Greenland flood basalt sequences has largely been restricted to chemical evidence for a temporal reduction in temperature during the syn-breakup interval (Tegner et al. 1998; Millett et al. 2017). A major volcanic hiatus is recorded between the pre-breakup and syn-breakup sequences of the Faroe Islands represented by the coal-bearing Prestfjall Formation (Passey and Jolley 2008; Passey 2014) which has been correlated to an equivalent volcanic hiatus in the East Greenland NAIP succession (Jolley and Whitham 2004). Although this major volcanic hiatus is well documented in the literature, a satisfactory explanation for why the NAIP volcanism switched off at this time has not been proposed to our knowledge.

The upper c. 1 km of the Beinivørð Formation reveals variably evolved tholeiitic compositions (Hald and Waagstein 1984; Jolley et al. 2012) and was termed ‘mixed magmas’ by Jolley et al. (2012). This interval also reveals evidence for reduced eruption rates linked to longer inter-eruption ecosystem development (Jolley et al. 2012), and therefore, independent of geochemical evidence, the magmatism of the FIBG appears to have slowed down in the lead up to the Prestfjall Formation regional hiatus. The volcanic facies also change distinctly across this boundary; from large-volume classic tabular lava flows in the upper Beinivørð Formation, to high-frequency, small-volume compound braided lava flow facies in the basal Malinstindur Formation, Fig. 1 d (Waagstein 1988; Passey and Bell 2007; Passey and Jolley 2008).

It is clear that the Beinivørð to Malinstindur Formation transition records, and may therefore give insights into, the origins of major magmatic pulsing within the FIBG, but it also potentially enables insights into a transition of significant importance to the evolution of the wider NAIP, namely the pre- to syn-breakup transition. In order to investigate this transition further, high precision major, trace, rare earth element (REE), and isotopic analyses are presented from new flow by flow sample transects spanning the uppermost c. 1.1 km of the Beinivørð Formation. Samples were collected from overlapping profiles on the western islands of Mykines and Vágur on the Faroe Islands, Fig. 1 e. These results are then compared with both new and published geochemical data from a repeat stratigraphic section on the southernmost island of Suðuroy (Fig. 1b) including data from the onshore borehole Lopra 1/1A and field profiles (Rasmussen and Noe-Nygaard

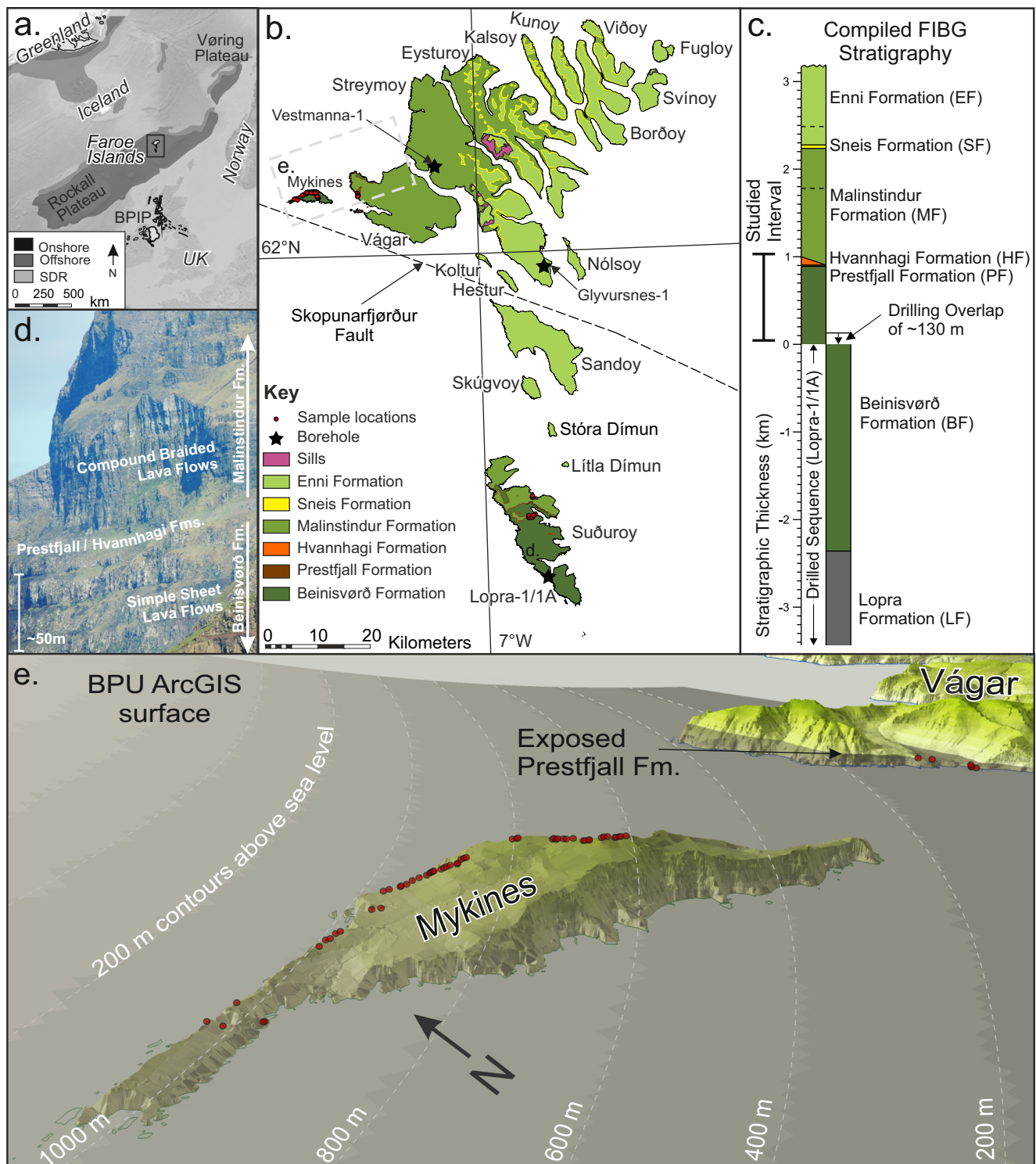


Fig. 1 **a** Simplified regional location map (after Larsen and Saunders 1998). **b** Geological map of the Faroe Islands showing the location of samples from this study (modified after Passey and Jolley 2008). **c** Compiled stratigraphy of the FIBG (after Passey and Jolley 2008). **d** Field picture of the major volcanic facies transition between the

Beinisdvøð and Malinstindur formations. **e** Map showing the 3D Beinisdvøð Prestfjall Unconformity (BPU) surface in ArcGIS (surface modified from Passey and Varming 2010) along with the detailed sample locations on Mykines and Vágur.

1970; Waagstein 1977; Hald and Waagstein 1984; Waagstein and Hald 1984; Waagstein 1988, 1997, 2006).

From these analyses, three clearly separated lava flow geochemical groups are identified, B1, B2 and B3, on the basis of

incompatible trace elements (e.g. Nb/Zr/Y) and REE character. The separate groups display limited Sr–Nd–Pb isotopic variations, and, therefore, the distinct inter-group REE variations are interpreted as differences in mantle melting, rather than changes in mantle source composition or contamination. Evidence from mantle melting calculations support a spinel-dominated mantle residue for group B1, whereas both group B2 and group B3 suggest a greater proportion of melting where garnet is present in the melting assemblage. These variations in pressure-dependent residual mantle mineralogy are interpreted to reflect changing pressure of initial melting most likely caused by changing mantle temperature. At the same time, group B1 magmas indicate slightly larger overall melt fraction which is interpreted as evidence for the onset of early rifting and lithospheric thinning to the north of the Faroe Islands.

The stratigraphic development of the different geochemical groups is striking, with the B1 lava flows being exclusively erupted at the very end of the Beinivörð Formation. This new evidence suggests that a transient reduction in mantle temperature led to the shutting down of FIBG magmatism synchronous with the onset of early rifting during the last stages of the previously defined pre-breakup sequence. For the first time, this study provides a petrological explanation for the diversity of geological changes that occurred during the pre- to syn-breakup transition of the FIBG. At the same time, this study demonstrates that fluctuations in mantle temperature coincided directly with the onset of continental breakup, and that any model for the province should incorporate mantle temperature pulsing, regardless of the preferred origin for temperature fluctuations at depth.

Methods

3D stratigraphic framework

The stratigraphy of the FIBG is tightly constrained within a 3D digital framework (Passey and Jolley 2008; Passey and Varming 2010) in which major marker horizons corresponding to regionally extensive sedimentary layers have been created using the spline surface interpolation tool in ArcGIS. This has allowed all the published lava flow geochemical data to be compiled into a single dataset constrained relative to the main regionally correlated surfaces making the FIBG one of the best spatially constrained LIP lava flow sequences (Passey 2004; Passey and Varming 2010). For the purposes of this study, only the BPU (Beinivörð–Prestfjall Unconformity) surface is utilized which traces a regionally extensive coal-bearing sedimentary sequence which separates the Beinivörð and Malinstindur formations. The new data presented in this contribution has been incorporated into the same framework, but with some minor updates to the surface used for GIS height extraction outlined below.

As noted by Passey and Varming (2010), the BPU surface prediction intercepts the top of Mykines, whereas no outcrop of the BPU has been found exposed on the island to date. This is explained by the increased dip angle on Mykines of 8° in the east increasing up to c. 20° in the west of the island in contrast to the lower dips of c. 3° along western Vágar, which is situated to the east of Mykines (Fig. 1e). With no location points on Mykines from which to interpolate a surface between the two islands, the surface of Passey and Varming (2010) has been manually modified to fit the available data (e.g. increasing the dip towards the west so there is no intersection with the summit of Mykines). The generated surface gives a realistic but non-unique estimate (Millett 2014) for the correlation between the islands (Fig. 1e). The BPU surface on Suðuroy, south of the Skopunarfjørður fault (Passey 2009), has not been altered from Passey and Varming (2010).

Sampling

For all the sample profiles, each individual lava flow was sampled within the constraints of exposure and access. For each sampled section, it is assessed that the vast majority of lava flows were sampled, however, where omissions occurred due to access, these are recorded in the stratigraphic columns presented for each section. Where sequences of compound lava flows were encountered, sampling was undertaken according to thickness, exposure and the presence of definite flow boundaries revealed by interbeds or reddened flow tops. Where substantial thicknesses of compound lava flows occurred, e.g. > 10 m, a sample was generally taken from the base and from the top of the sequence. Sampling of tabular lava flows was undertaken from the freshest accessible part of each flow, generally comprising the core of the flow between c. 1 m above flow base and 2–3 m below the flow top depending on flow size and degree of vesiculation.

GPS points were collected in the European Datum 1950 (ED50) coordinate system for samples and flow boundaries. Elevations were extracted from a high-resolution DEM of the Faroe Islands for consistency. All reported stratigraphic heights were calculated by subtracting the sample elevation from the updated BPU spline surface height (Passey and Varming 2010; Millett 2014) accounting for the surface extracted dip angle at each sample location (see data provided as Online Resource 1).

Geochemical analyses

In total, 69 samples were analysed for this study. Representative whole-rock chemical analyses are presented in Table 1 and all data are available in the Online Resource 2. All samples were crushed in a fly press followed by powdering in an agate tema-mill at the University of Aberdeen, Aberdeen, UK. Powders were analysed for major and trace

Table 1 Representative geochemical data for the Beimsisvørð Formation. For full analyses, see Online Resource 2–3

Formation	Beimsisvørð										
	SUI2-1-10	SUI2-1-7	MK12-1-4	MK12-1-10	MK-1-1	MK-6-16	SUI2-1-7	MK-3-1	MK-4-4	MK-6-20	SUI2-1-3
Sample	SUI2-1-10	SUI2-1-7	MK12-1-4	MK12-1-10	MK-1-1	MK-6-16	SUI2-1-7	MK-3-1	MK-4-4	MK-6-20	SUI2-1-3
Island	Stuðuroy	Stuðuroy	Mykines	Mykines	Mykines	Mykines	Stuðuroy	Mykines	Mykines	Mykines	Stuðuroy
Depth to BPU (m)	–5	–98	–158	–48	–1127	–620	–98	–1077	–967	–554	–153
Group	B1	B2	B1	B1	B2	B2	B2	B3	B3	B3	Trans.
XRF majors	48.68	47.94	47.77	49.04	48.35	48.33	47.43	46.92	45.16	46.59	
SiO ₂	1.65	1.57	1.21	2.35	3.45	2.03	2.59	3.48	4.27	2.68	
TiO ₂	14.97	13.92	13.62	13.62	13.92	13.92	14.26	12.82	12.18	13.92	
Al ₂ O ₃	13.38	14.15	11.30	14.58	16.96	13.43	15.17	16.83	17.93	14.47	
Fe ₂ O ₃	0.21	0.23	0.18	0.21	0.23	0.19	0.22	0.22	0.26	0.20	
MnO	5.88	6.95	6.68	6.01	4.69	6.51	6.23	4.97	4.75	6.82	
MgO	11.41	10.97	12.62	11.18	8.99	11.55	10.95	9.66	9.71	10.95	
CaO	2.26	2.09	1.93	2.54	2.69	2.10	2.74	2.62	3.02	2.19	
Na ₂ O	0.22	0.16	0.28	0.28	0.84	0.20	0.51	0.54	0.62	0.35	
K ₂ O	0.17	0.17	0.12	0.23	0.37	0.17	0.27	0.39	0.50	0.26	
P ₂ O ₅	0.43	1.13	1.22	0.63	0.00	0.61	0.49	0.96	1.86	1.07	
LOI	99.27	99.29	99.49	100.66	98.91	99.05	100.86	99.42	100.27	99.50	
Total	5.6	0.7	0.7	5.8	18.2	0.9	8.7	9.1	6.0	2.4	
XRF traces	210.0	175.6	218.9	289.7	307.5	275.8	357.5	396.4	390.7	289.1	
Rb	29.9	33.5	27.7	30.9	44.2	27.4	24.8	40.0	48.6	33.4	
Sr	103.5	98.5	73.3	139.2	244.2	112.9	143.0	237.1	284.4	152.2	
Zr	10.4	10.6	7.5	10.2	19.3	9.1	14.8	23.5	31.1	15.8	
Nb	106.3	95.2	66.9	75.2	209.3	79.6	125.1	228.8	249.8	155.8	
Ba	3.7	3.8	0.0	6.0	9.5	2.2	4.8	6.2	6.8	2.6	
Pb	0.7	1.6	1.1	3.1	3.2	2.5	5.4	3.3	1.6	2.9	
Th	1.6	0.0	2.4	0.0	0.6	–0.2	–0.4	0.0	1.2	0.9	
U	39.5	45.6	44.0	35.3	32.9	37.1	30.1	29.3	29.3	36.5	
Sc	354.6	375.0	283.5	372.2	421.9	334.5	361.0	383.0	397.9	335.7	
V	46.4	96.4	157.2	157.1	48.7	174.4	61.8	27.0	31.5	121.4	
Cr	40.4	44.1	39.6	43.7	37.9	46.9	44.4	39.1	36.6	41.2	
Co	49.8	66.3	70.1	85.0	44.0	82.3	82.3	52.4	48.9	83.7	
Ni	153.4	93.7	87.1	196.1	126.7	142.6	191.8	232.5	280.5	139.5	
Cu	86.5	91.8	66.9	99.7	126.0	85.5	84.3	112.3	125.9	87.7	
Zn	19.9	18.2	17.8	22.1	27.8	20.5	23.6	25.5	26.4	23.1	
ICP-MS REE	8.46	8.36	5.63	10.26	20.76	8.66	14.46	25.47	29.68	13.64	
La	19.98	19.39	13.45	26.70	50.37	36.00	36.00	59.46	70.52	32.96	
Ce	2.86	2.78	1.99	3.89	7.28	3.30	5.05	8.10	9.76	4.79	
Pr	13.30	13.00	9.58	18.29	32.88	15.80	22.09	34.63	42.78	22.00	
Nd	3.78	3.74	2.84	5.12	8.75	4.47	5.40	8.37	10.45	5.89	
Sm	1.34	1.33	1.06	1.79	2.75	1.60	1.83	2.67	3.28	1.93	
Eu	4.56	4.66	3.50	5.71	9.06	5.05	5.51	8.43	10.59	6.37	
Gd	0.78	0.83	0.61	0.91	1.43	0.84	0.82	1.29	1.60	1.02	
Tb	4.94	5.28	3.80	5.35	8.20	4.81	4.66	7.25	9.03	5.98	
Dy	1.06	1.16	0.83	1.06	1.61	0.99	0.91	1.41	1.75	1.23	
Ho	2.99	3.36	2.36	2.85	4.28	2.63	2.39	3.73	4.64	3.27	
Er	2.71	3.11	2.17	2.37	3.52	2.17	1.93	3.08	3.81	2.80	
Yb	0.41	0.46	0.31	0.34	0.49	0.30	0.28	0.43	0.52	0.40	
Lu											

elements on an ARL 8420+ dual goniometer wavelength dispersive XRF spectrometer at the Open University XRF laboratory, Milton Keynes, UK. Major elements were determined on fused glass beads prepared from ignited powders mixed with a lithium metaborate/tetraborate flux following the analytical procedures outlined in Ramsey et al. (1995). In-house standards (WS-E and OU-3) were run at regular intervals to ensure analytical precision and accuracy (see Online Resource 2). Loss on ignition was determined after heating to 1000 °C. Trace elements were analysed on pressed powder pellets prepared after the method of Watson (1996). Reference standards (BHVO-1, DNC-1, QLO-1 and W-2) were run at regular intervals to ensure analytical precision and accuracy (see Online Resource 2). All presented major element XRF analyses are normalised to 100% on a volatile-free basis with a fixed oxidation ratio of $\text{Fe}_2\text{O}_3/\text{FeO} = 0.15$.

Inductively coupled plasma mass spectrometry (ICP-MS) analysis was conducted on a subset of 20 samples spanning the range of trace element-defined compositions at the Open University ICP-MS laboratory on an Agilent 7500 s ICPMS machine (see Online Resource 3). The analyses were run calibrated against the reference materials set (BIR-1, BHVO-2, W-2, DNC-1 and AGV-1) and undertaken in a single run. A monitor block using BHVO-2 was also run every five analyses which was used to drift correct along with one of the samples (GD-4-2) to check that the drift correction worked as well as a rinse blank which ran without any issues. The precision for all elements gauged by RSD % is better than 2% for the BHVO-2 monitor block and for the GD-4-2 sample except for the elements Cu (7.27%) and Cs (2.87%). Accuracy is assessed by comparing the average analysis for the BHVO-2 monitor with USGS published values for the standard. Determinations of all elements display accuracy better than 5% except for Li, Cr, Rb, Sn and Ho which show accuracy better than 10%.

Electron-micro-probe analysis

All mineral chemistry data was acquired with a MICROSCAN MK5 using a Link Analytical AN10/25S system at the University of Aberdeen. Analyses were acquired and processed using the ZAF4/FLS program. The standard beam diameter is approximately 5 μm with analysis of olivine and pyroxene undertaken with a 200-s lifetime whilst a count time of 150 s was used for plagioclase analyses. Detection limits for minor elements such as Ti, Al and Cr are typically c. 0.15 wt% or better for olivine and pyroxene analyses. All raw and recalculated mineral chemistry data is presented within the Online Resources 4–6.

Isotopic analysis

Nine representative samples, comprising some of the least fractionated and freshest basalt samples as defined by

trace elements, were analysed for Sr-, Nd- and Pb-isotope geochemical compositions at the East Kilbride Scottish Universities Environmental Research Centre (SUERC). Samples were prepared and analysed following the standard protocols used at SUERC (see also Online Resource 7). Samples were digested in PFA Teflon (savillex) beakers on a hotplate at 140–150 °C using ultrapure HF, HNO_3 and HCl steps for Sr and Nd extraction and HBr-based anion exchange method for Pb extraction. Analyses of $^{87}\text{Sr}/^{86}\text{Sr}$ and $^{143}\text{Nd}/^{144}\text{Nd}$ were carried out on a VG sector 54-30 thermal ionisation mass spectrometer (TIMS) in a multidynamic mode using exponential corrections for mass fractionation and $^{86}\text{Sr}/^{88}\text{Sr} = 0.1194$, and $^{144}\text{Nd}/^{146}\text{Nd} = 0.7219$. Pb-isotope compositions were analysed in a Micromass IsoProbe, MC-ICP-MS, using an Elemental Scientific Inc. 100 $\mu\text{l min}^{-1}$ PFA nebuliser and an ESI APEX-Q inlet system, following the methodology described by Ellam (2006). From the selected samples, all nine have produced results for $^{87}\text{Sr}/^{86}\text{Sr}$, eight produced results for $^{143}\text{Nd}/^{144}\text{Nd}$ and only six samples produced results for Pb isotopes. A detailed description of sample preparation and analytical methods is provided in the Online Resource 7 and summarized in Table 2.

Results

Facies development

All samples taken from the Mykines profile represent sub-aerial lava flow facies with no evidence of lava-water interaction or lava sediment interaction other than minor loading of interbed sediments. Interbedded sedimentary units representing soils developed during eruption hiatuses and/or ashfall deposits are abundant in the section; however, they are generally only a few centimetres in thickness but may reach thicknesses >10 m in a few cases towards the top of the sample sequence on Mykines (Fig. 2). The thickness of interbeds varies substantially laterally as a function of lava flow field palaeotopography and lava flow facies distribution (e.g. Fig. 2d). The measured interbed facies comprise <3% of the logged stratigraphy; however, this is a minimum estimate due to typically poorer exposure and in-weathering of the softer interbed facies between the lava flows.

The sub-aerial volcanic facies can be broadly split into three eruptive lava flow types namely classic tabular, compound braided and ponded lava flow facies (Lyle 2000; Jerram 2002; Passey and Bell 2007). Examples of each lava flow type are displayed in Fig. 2. A composite facies log of the Mykines profile based on a combination of field data and height interpolation from the ArcGIS BPU surface is presented in Fig. 3. The facies of the Mykines profile is heavily dominated by tabular

Table 2 Sr, Nd and Pb isotopic analyses for studied FIBG samples

Sample ID. Group	MK12-1-6 B1	SU12-1-10 B1	GD-1-6 B1	MK-4-4 B3	MK-2-3 B3	MK-3-1 B3	MK-5-2 B2	MK-6-7 B2	MK-1-1 B2
$^{87}\text{Sr}/^{86}\text{Sr}$	0.7036	0.7035	0.7037	0.7037	0.7036	0.7034	0.7034	0.7036	0.7036
Rb/Sr	0.0518	0.0164	0.0123	0.0667	0.0666	0.0652	0.0147	0.0134	0.0605
$^{87}\text{Sr}/^{86}\text{Sr}_{56\text{Ma}}$	0.7035	0.7035	0.7037	0.7037	0.7036	0.7033	0.7034	0.7036	0.7036
$^{143}\text{Nd}/^{144}\text{Nd}$	–	0.5130	0.5129	0.5129	0.5129	0.5130	0.5129	0.5130	0.5129
$^{147}\text{Sm}/^{144}\text{Nd}$	–	0.1717	0.1703	0.1512	0.1443	0.1378	0.1672	0.1711	0.1691
$^{143}\text{Nd}/^{144}\text{Nd}_{56\text{Ma}}$	–	0.5129	0.5129	0.5129	0.5129	0.5129	0.5129	0.5129	0.5129
$\epsilon\text{Nd}_{56\text{Ma}}$	–	6.3635	6.0806	5.5537	6.4026	6.5665	5.7319	6.4069	5.8552
$^{206}\text{Pb}/^{204}\text{Pb}$	–	–	17.9899	17.9642	18.1235	18.1017	–	18.0934	18.1100
$^{207}\text{Pb}/^{204}\text{Pb}$	–	–	15.4163	15.4117	15.4365	15.4418	–	15.4522	15.4608
$^{208}\text{Pb}/^{204}\text{Pb}$	–	–	37.8551	37.9540	37.9827	37.9180	–	37.9520	37.9596

Initial Sr and Nd isotopic ratios were recalculated to 56 Ma using $\lambda = 1.42\text{E}-11$ and $\lambda = 6.54\text{E}-12$, respectively

sheet flows displaying crude prismatic jointing for just under 75% of the exposed section. Small compound flow facies intervals (e.g. at – 1120 m, – 530 m and – 360 m) are present, but never reach thicknesses above c. 25 m in total and only represent c. 7% of the section. Columnar ponded lava flows represent c. 15% of the succession, but are only well developed at the very base of the succession and then again at c. – 1400 m. The Mykines sequence is, therefore, dominated by high effusion rate classic tabular lava flows, which were commonly succeeded by significant time gaps during which time sedimentary redbeds had time to form. This facies-type development is consistent with the high effusion low-frequency sequence development described from the upper Beinisdvörð section on Suðuroy (Jolley et al. 2012).

Short sample profiles were also collected from Vágur and Suðuroy (Fig. 3). The sampled sections leading up to the Prestfjall Formation both consist of dominantly large classic tabular lava flows separated, in the majority of cases, by bright red interbeds of variable thickness (Passey and Bell 2007; Passey and Jolley 2008). Thick ponded columnar flows displaying colonnade and entablature multi-tiered features are also present towards the top of the sequence on Suðuroy (Passey and Jolley 2008). Above the last lava flow of the Beinisdvörð Formation, the Prestfjall Formation sedimentary interval comprises a clay-rich sequence up to c. 15 m thick containing coal units that have been mined in several locations on Suðuroy (Passey and Jolley 2008). The Prestfjall Formation is overlain by the syn-eruptive volcanoclastic to pyroclastic Hvannhagi Formation which locally reaches c. 50 m thick but is highly laterally heterogeneous and has been interpreted as geochemically linked to the overlying Malinstindur Formation (Waagstein 1988). The first few hundred meters of the Malinstindur Formation comprises a sequence of exclusively compound braided lava flow facies in marked contrast to the underlying Beinisdvörð Formation (Passey and Jolley 2008).

Geochemistry of the lava flows

The general chemistry of the Beinisdvörð Formation lava flows has been reported previously (Gariépy et al. 1983; Hald and Waagstein 1984; Waagstein 1988; Passey and Jolley 2008; Jolley et al. 2012). LOI (loss on ignition) of the samples analysed within this study is uniformly low, with no samples showing LOI > 1.5 wt% which is consistent with the generally fresh nature of the collected samples. Major and trace element variations in the Beinisdvörð Formation lava flows are summarized in Figs. 4 and 5. The lava flows have MgO contents in the range 4.5–7.8 wt% and all are classified as basalts in terms of the total alkalis-silica diagram of Le Maitre et al. (2002) and tholeiitic by the scheme of Irvine and Baragar (1971). TiO_2 , FeO^T , Na_2O and P_2O_5 correlate negatively, and Al_2O_3 and CaO correlate positively with MgO content (Fig. 4). The latter positive correlations are indicative of a role for plagioclase \pm augite in the crystallizing assemblage for the entire compositional range analysed. Data are scattered on a plot of SiO_2 versus MgO (not shown) with no coherent variations being evident. The lava flows are dominantly olivine tholeiites in terms of their CIPW norms with a small number of evolved samples containing up to 5% normative quartz.

Cr and Ni exhibit a general increase with increasing MgO, whereas more incompatible elements such as Zr exhibit progressive decreases with increasing MgO content. For Sr, two lineages are evident (Fig. 4) one with Sr < 250 ppm and one with Sr in the range 250–400 ppm. Within these two ranges, Sr is relatively consistent across a broad range of MgO reflecting a strontium melt/rock partition coefficient (D_{Sr}) of ~ 1 .

Zr, Nb and Y are particularly useful for investigating the petrogenesis of tholeiitic magmas because they are unaffected by alteration and are all incompatible with respect to the main crystallizing basaltic phases (Morrison 1978; Larsen and Saunders 1998; Fitton et al. 1998). These elements may,

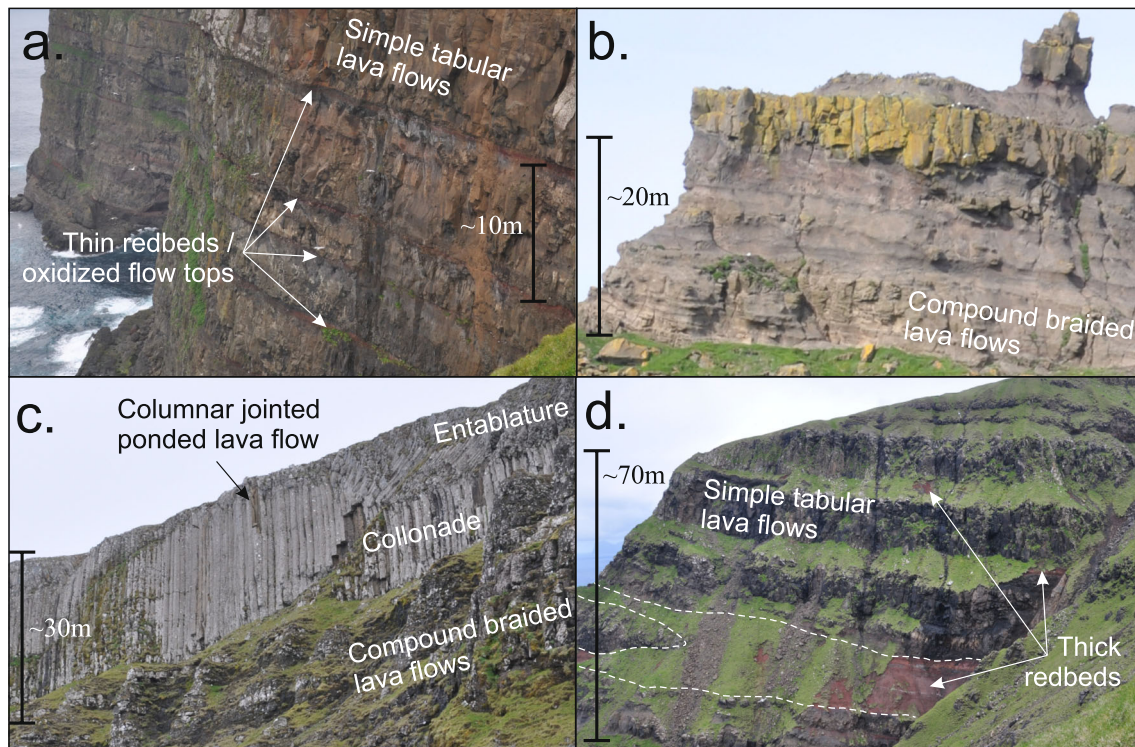


Fig. 2 Volcanic facies from Mykines. **a** Stacked classic tabular laterally continuous lava flow facies looking NE to Havnarfles. **b** Compound braided lava flow facies displaying abundant laterally discontinuous lobes and flow crusts above the bridge to Mykineshólmur. **c** Ponded

columnar lava flow facies at Kálvadalur. **d** Reddened interbeds showing lateral bifurcation and variations in thickness due to a lava flow pinching out, North facing side of Kálvadalur, Mykines

however, show minor variations of incompatibility in the order $Nb > Zr > Y$ where pyroxene is an important constituent. Covariations between Zr, Y and Nb have been used to subdivide the lava flows into three distinct groups, B1, B2 and B3 (Fig. 5). Groups B1 and B3 are indistinguishable in terms of Zr/Nb ratio c. 9.7 each displaying linear regressions intersecting the origin consistent with fractional crystallization, whereas B2 displays a distinct array with Zr/Nb of c. 12.7, also intersecting the origin. Group B1 displays Zr/Y in the range of 2.6 to 3.7 (Fig. 5) and is clearly separated from B3 lava flows which have Zr/Y ratios of 5.4 to 6.5 whilst group B2 lava flows display Zr/Y ratios of 4.0 to 5.6, intermediate between B1 and B3. Group B1 lava flows also represent the lowest TiO_2 (1.4–2.2 wt%) lava flows in the stratigraphy. Outside of the three clear groups, two samples from the 69 lava flow analyses do not fit clearly into any of the groups and have been termed transitional. These samples are regarded as most likely comprising the product of sub-surface magma mixing within the shallow crust.

Covariations between Zr and Zr/Y exhibit slight positive slopes and indicate either a slightly higher D_Y than D_{Zr} during crystallization including pyroxene, or mixing between liquids with differing Zr/Y. Covariations between Zr and Zr/Sr define steep positive trends for each group of lava flows which, along with the Sr versus MgO correlation (Fig. 4), suggests that $D_{Zr} < D_{Sr} \sim 1$ during crystallization. Crystallization of olivine and

augite would produce near-horizontal arrays in Fig. 5d, whereas fractionation of plagioclase feldspar would cause increasing Zr/Sr with increasing Zr because $D_{Zr} < D_{Sr}$ for the assemblage $L + Ol + Pl + Cpx$.

All analysed samples are light rare earth element (LREE) enriched ($[La/Yb]_N = 1.67\text{--}5.93$; Fig. 6) with no noticeable Eu anomalies. LREE enrichment increases in the order B1 through to B3 implying decreasing extents of melting in the same order. Groups B2 and B3 lava flows have shallower normalized profiles from La to Sm ($[La/Sm]_N = 1.2\text{--}1.8$) compared to those for elements Sm to Yb ($[Sm/Yb]_N = 2.0\text{--}3.2$).

Multi-element variation diagrams normalized to primordial mantle of Sun and McDonough (1989) exhibit convex-upward patterns with a noticeable dip at phosphorus likely resulting from apatite crystallization (Fig. 7). La/Nb (0.76–1.0) and Th/Nb (0.07–0.10) are within the ranges expected for mid-ocean ridge basalt (MORB) or melts of primitive mantle (La/Nb \sim 1.0; Th/Nb = 0.05–0.11). None of the Beinisvörð Formation lava flows have the high La/Nb and Th/Nb ratios that characterise other NAIP lava flows that have undergone significant interaction with ancient continental crust (up to 6 and 0.7 respectively; Hole et al. 2015; Pedersen et al. 2017). Elevated Ba/Zr > 1 is observed for a small number of samples in groups B1 and B2, a feature that and has previously been linked to crustal contamination for samples from ODP Legs 152 and 163 (Larsen et al. 1998;

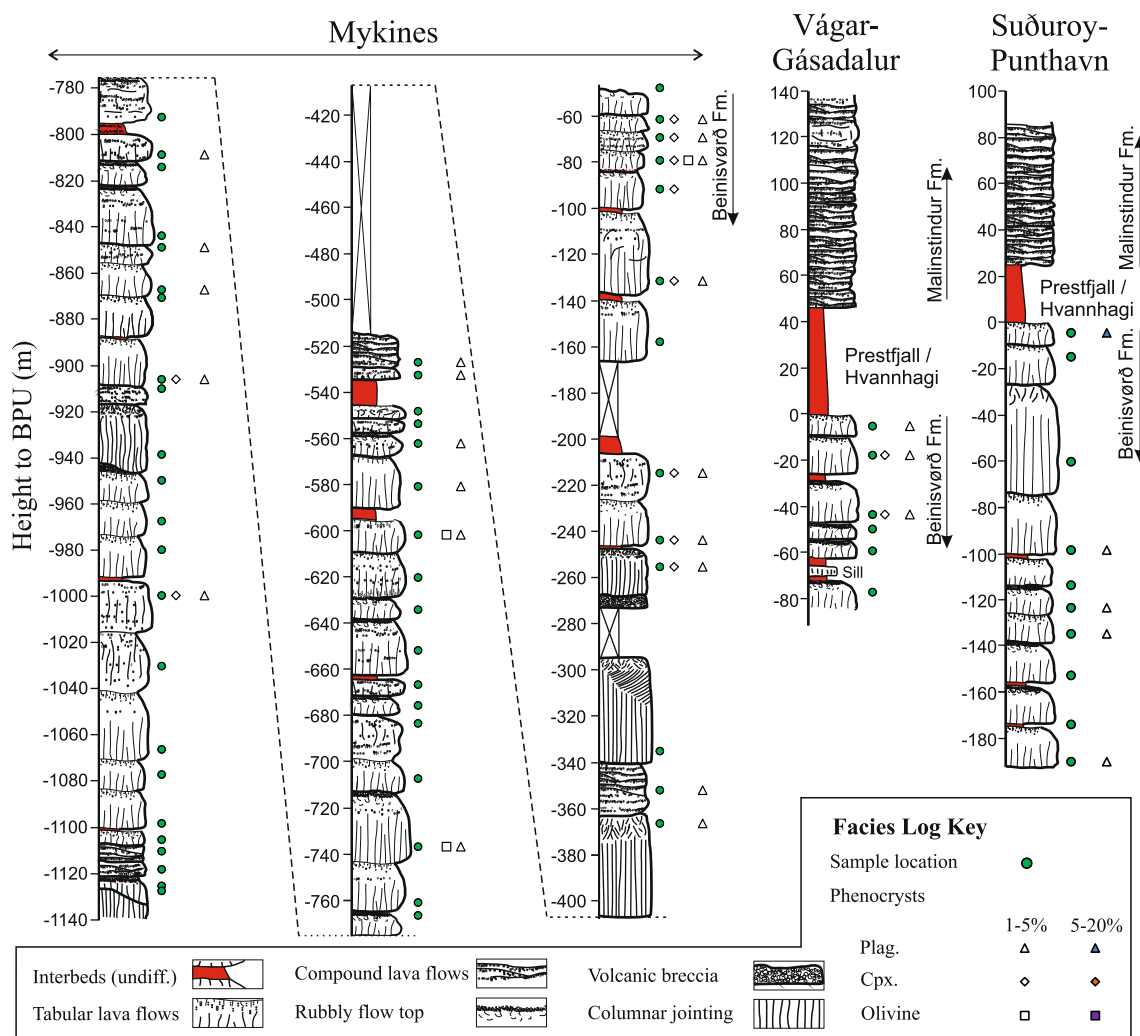


Fig. 3 Composite schematic facies logs through the Mykines, Vágar and Suðuroy sampled profiles showing broad facies type, sample sites and interbed locations. Phenocrysts types and abundance estimated from

petrographic analysis are also indicated. Exposure gaps or inaccessible intervals are denoted with a cross

Fitton et al. 1998). However, with the vast majority of the analysed FIBG samples revealing Ba/Zr <1, only very minor degrees of crustal contamination are supported in the analysed samples.

Mineral chemistry

The Beinisvørð Formation samples collected for this study are aphyric to weakly plagioclase/clinopyroxene aphyric (generally <5%) with typically fine to very-fine-grained groundmass of clinopyroxene, plagioclase, Fe oxides and rare olivine. Pyroxenes display ophitic textures in places and plagioclase occurs as either individual phenocrysts or glomerocrysts with common sieve textures (see Online Resource 8). Olivine only occurs in six out of the 69 sampled lava flows as rare micro-phenocrysts or as a groundmass phase. Fo content varies from 30.0 to 70.2 for a range of whole-rock Mg# = 0.365–0.489.

None of the analysed olivines approach equilibrium with their host rocks, all olivines having a lower Fo content than that predicted from host rock Mg#. This implies that olivine either crystallized from a late-stage residual liquid or represents xenocrysts derived from more evolved magmas in the fractionation series.

The compositions of plagioclase feldspar and augite phenocryst cores exhibit systematic variations with the major element composition of their host rocks. Anorthite content of plagioclase feldspar and Mg# of augite increases with increasing Mg# content of the host rock regardless of which trace element group the lava flows belong to, e.g. Fig. 8. The highest Mg# augite in each sample falls close to the equilibrium condition of $k_{D[Fe-Mg]}^{Cpx-L} = 0.27 \pm 0.03$ (Putirka 2008). Sample SU12-1-7 contains plagioclase feldspar which falls above the main trend to higher An at a given Mg# than the remainder of the lava flows, suggesting plagioclase feldspar phenocrysts are

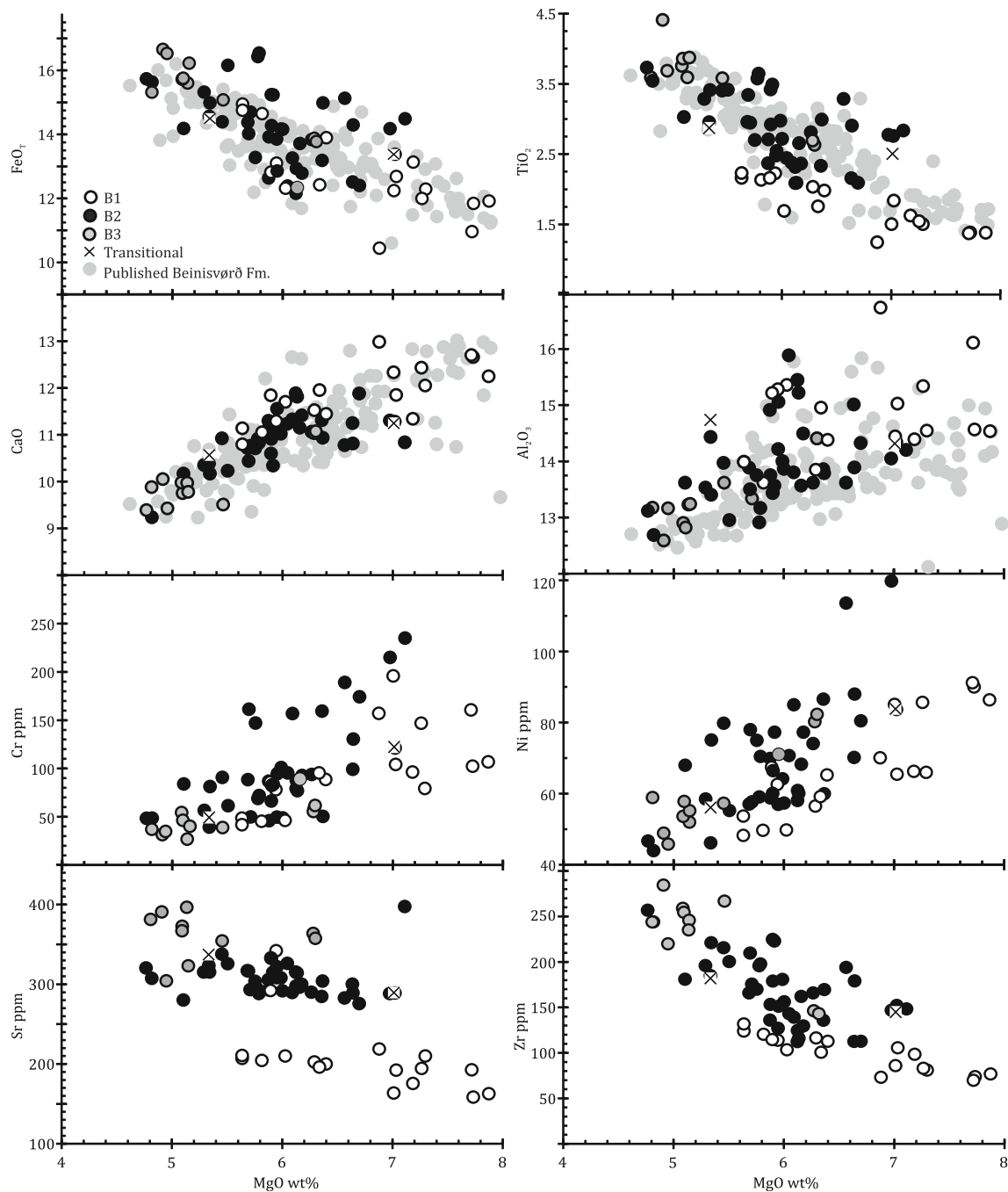


Fig. 4 Selected major and trace elements versus MgO for Beinisvörð Formation lava flows analysed during this study. The grey dots display the range of compositions from Hald and Waagstein (1984) and Waagstein and Hald (1984)

accumulative in this sample. These relationships suggest that the major element compositions of Beinisvörð Formation lava flows are controlled by crystallization of the observed phenocryst phases.

In contrast, the base of the Malinstindur Formation is dominated by olivine to lesser clinopyroxene porphyritic basalt and picrites with the samples commonly becoming densely olivine phyric with accumulative olivine (Passey and Jolley 2008; Jolley et al. 2012).

Isotope geochemistry

Of the nine analysed samples, robust determinations were achieved for nine $^{87}\text{Sr}/^{86}\text{Sr}_{56} = 0.70334\text{--}0.70370$, eight $\varepsilon\text{Nd}_{56} = 5.2\text{--}6.2$ and six $^{206}\text{Pb}/^{204}\text{Pb} = 17.96\text{--}18.12$ samples spanning the three main groups (Fig. 9). The compositions for all groups are similar and plot within the range for those given by Gariépy et al. (1983) for ‘Lower Series Lavas’, which is equivalent to the modern Beinisvörð Formation nomenclature (Passey

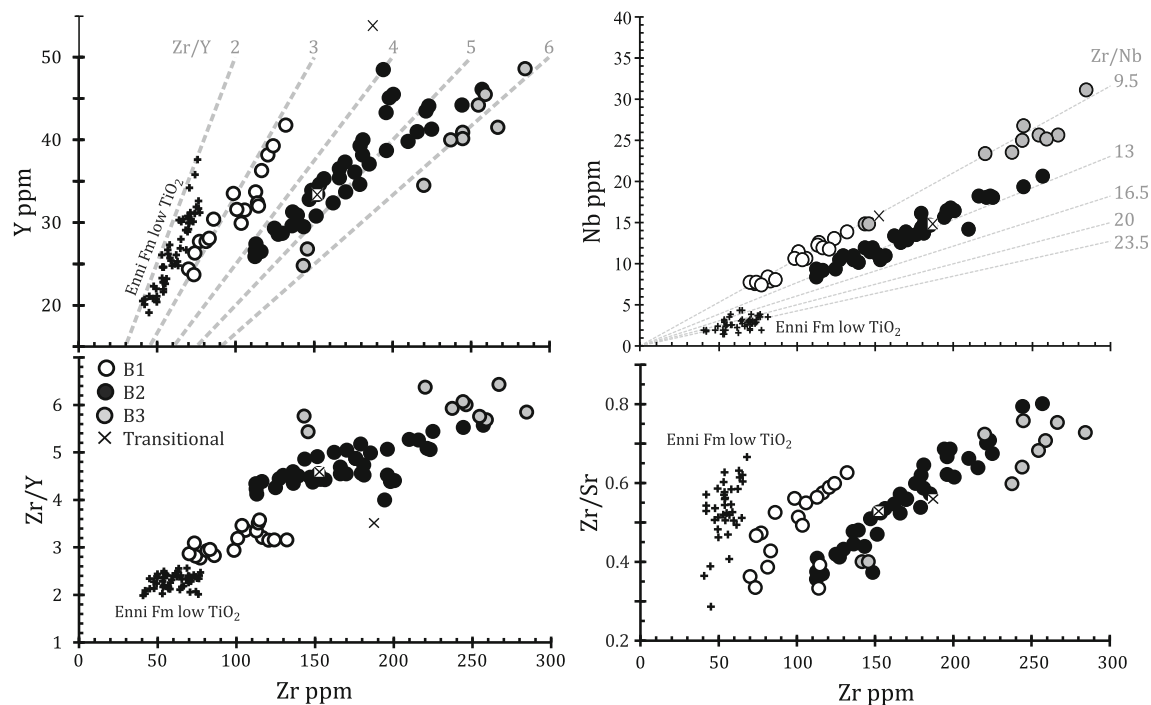


Fig. 5 Incompatible trace elements Y and Nb versus Zr along with the Zr/Y and Zr/Sr versus Zr for Beinisvørð Formation lava flows. The field for Enni Formation Low-Ti lava flows is from Millett et al. (2017)

and Jolley 2008). The Beinisvørð Formation lava flows have some of the most radiogenic Sr and unradiogenic Nd-isotopic compositions of any Faroese lava flows and fall at the extreme end of the Faroe Islands array shown in Fig. 9. Pb-isotopic compositions scatter around the northern hemisphere reference line (NHRL) and at the low $^{206}\text{Pb}/^{204}\text{Pb}$ end of the Iceland array (Fig. 9(b)). On a plot of $^{206}\text{Pb}/^{204}\text{Pb}$ versus ϵNd_{56} , Beinisvørð Formation lava flows plot at lower $^{206}\text{Pb}/^{204}\text{Pb}$ and lower ϵNd_{56} than lava flows defining the Iceland array and overlap with the compositions of other Faroe Islands lava flows.

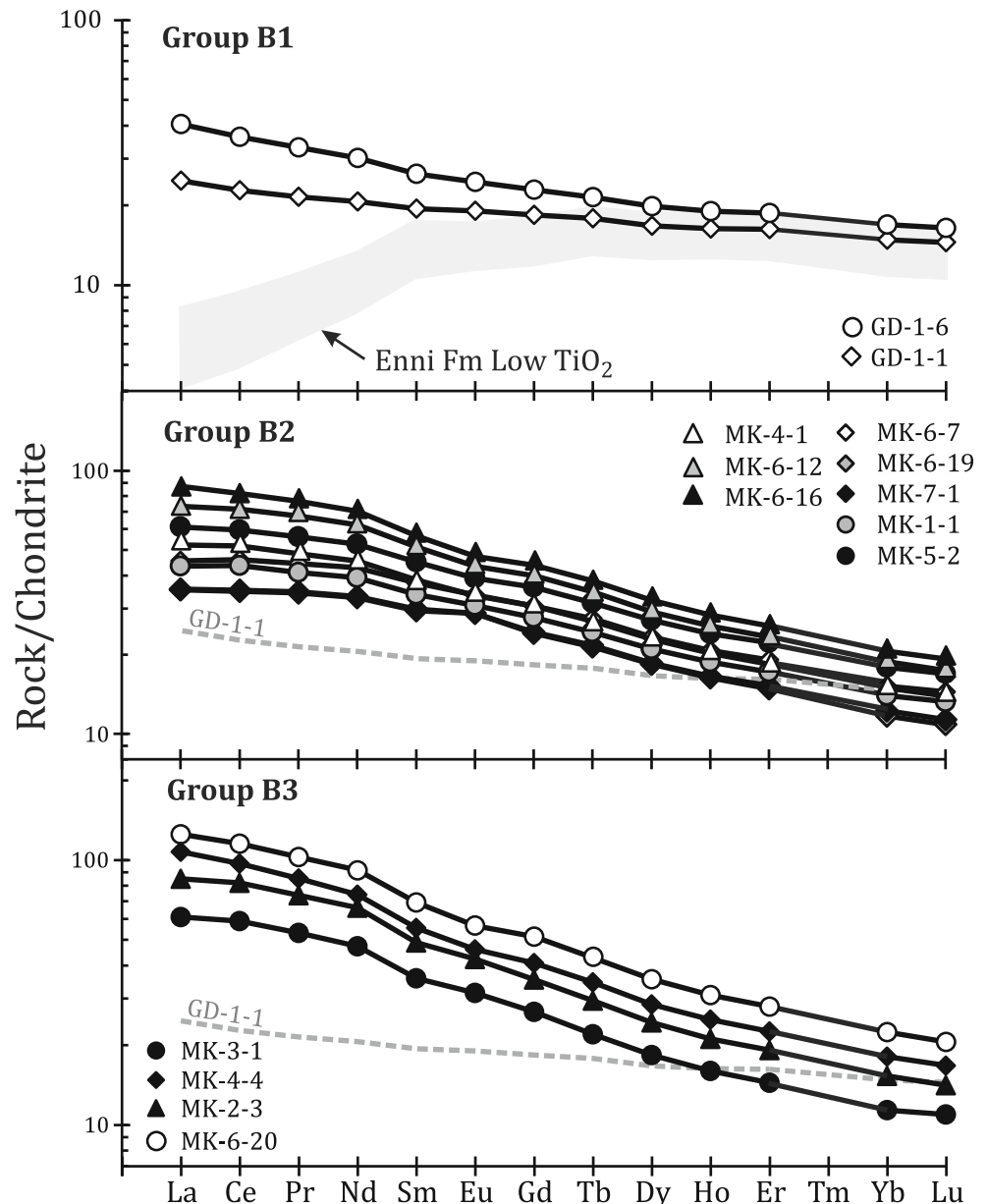
Whereas some Beinisvørð Formation lava flows have Sr-, Nd- and Pb-isotopic compositions that are within the range for Iceland, the distribution of data points away from the Iceland array towards both lower ϵNd_{56} and $^{206}\text{Pb}/^{204}\text{Pb}$ (Fig. 9) is consistent with small amounts of contamination by a local crustal or lithospheric mantle component potentially comprising Archean amphibolite or granulite gneiss as proposed by Søager and Holm (2011). The low ϵNd_{56} component does not appear to share the radiogenic Pb compositions seen within lava flows from Oraefajökull, Iceland, which has been postulated to be a felsic component in the Iceland crust (Torsvik et al. 2015). Interaction between mantle-derived magmas and ancient continental crust is well documented for the BPIP (e.g. Thompson 1982; Hole et al. 2015; Ishizuka et al. 2017) and is always accompanied by increases in La/Nb (up to 6) and Th/Nb (up to 0.7) compared to uncontaminated lava flows, features which are not observed in the Beinisvørð Formation lava flows. This contrast in composition is also visible in isotopic data, where minor interactions (less than 5% AFC) between basaltic magmas and ancient continental

crust shift $^{143}\text{Nd}/^{144}\text{Nd}$ and Pb isotopes towards lower ratios (Kerr et al. 1995; Hole et al. 2015). Consequently, the amount of interaction between an old crustal source with elevated La/Nb and/or Th/Nb and the Beinisvørð Formation lava flows appears minimal compared to the total range seen in NAIP lava flows and indeed also in relation to the most contaminated FIBG magmas (Søager and Holm 2011). This along with the limited inter-group variations implies that trace element variations, and particularly those involving the REE and HFSE, are dominated by melting and crystallization processes rather than by crustal contamination or changes in mantle source.

Geochemical development and correlation

In Fig. 10, the sample profiles from this study are presented relative to the updated BPU surface with the facies, sample locations, phenocrysts assemblages and chemical groups highlighted. Based on the updated BPU surface, the Mykines and Vágur sample profiles overlap supporting the premise that a complete stratigraphic sequence has been sampled in the north western study area. In addition to the new samples, a composite profile for the sampled profile of Hald and Waagstein (1984) is also presented. The facies log for the sampled lava flows is derived from a quick field log by the authors in a similar, but not identical, location to the published samples and should therefore be regarded as indicative only. The chemical compositions of the published data have been separated using the same criteria as in the present study and reveal a broadly similar compositional range albeit with more scatter (see Online Resource 9). In

Fig. 6 Chondrite normalized REE patterns for Beinissvörð Formation lava flows analysed in this study. The field for Enni Formation Low-Ti lava flows is from Millett et al. (2017) and Søger and Holm (2011)



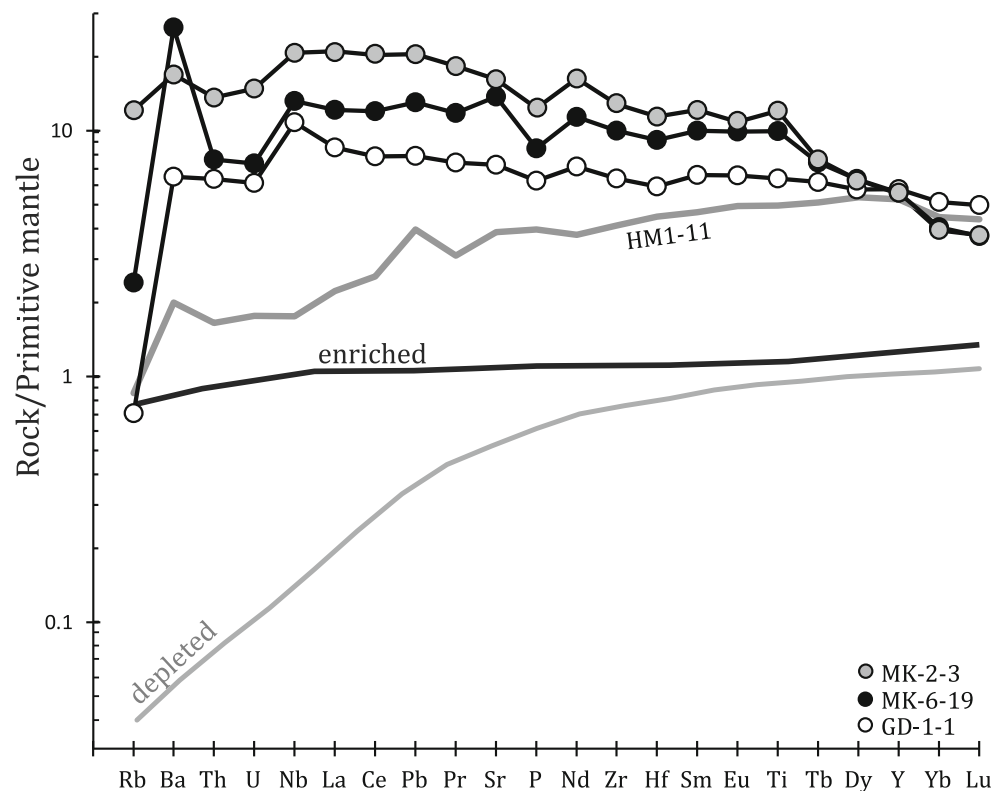
particular, the identification of group B2 and B3 samples between c. –100 and –220 m in the published data is regarded as tentative due to significant scatter and overlap.

What is immediately clear from Fig. 10 is that the different chemical groups of the Beinissvörð Formation are not randomly distributed. The B1 lava flows are entirely restricted to the last few flows of the Beinissvörð Formation and occur at this level in both the Mykines/Vágar succession and in the Suðuroy succession separated by c. 75 km. The B1 lava flows appear to be volumetrically more important in the Mykines/Vágar succession revealing a thickening of the sequence to the NNW. These flows represent the last expression of the Beinissvörð Formation volcanism and equivalently are the last eruptions of repeated stacked high-volume classic tabular lava flows within the FIBG. Packages of B3 lava flows occur as

discrete intervals within the B2 dominated sequence, with the main occurrences located below c. –900 and –1100 m in the Mykines and Suðuroy sequences respectively. B2 and B3 lava flows were clearly fed by coexisting magmatic plumbing systems which were replaced by B1 magmatism during the last eruptive phase of the Beinissvörð Formation. The two Transitional lava flow samples occur at the base of the Mykines section between B2 and B3 intervals, and within the B2 dominated short Suðuroy sampled section.

There appears to be no systematic correlation between the separate magma groups and facies types other than the increased number and thickness of interbeds towards the top of the Beinissvörð Formation sequence and a general dominance of large simple tabular lava flows. This is in stark contrast to the overlying Malinstindur Formation which comprises exclusively

Fig. 7 Incompatible element abundances normalized to the primitive mantle composition of Sun and McDonough (1989) for representative samples of groups B1–3 Beinivörð Formation lava flows. The grey lines labelled ‘depleted’ is the model composition of north Atlantic MORB source asthenosphere for MORB out with the influence of the Iceland thermo-chemical anomaly at 53–60°N (Murton et al. 2002, as used in Hole et al. 2015). The ‘enriched’ pattern is the proposed composition from which Beinivörð Formation lava flows were derived. See text for discussion



compound braided lava facies. No clear and systematic chemical evolution with stratigraphic height is observed internally within each group (Fig. 10 and Online Resource 9) such as those identified by Jolley et al. (2012) from the deeper Lopra-1/1A borehole. This suggests that the plumbing system for each group underwent fractionation and replenishment erupting variably differentiated magmas from initially similar melt batches (Sparks et al. 2019). The transitional compositions alongside scatter within each group are likely the response of variable degrees of melt batch mixing within the complex multi-tiered plumbing system.

B1 lava flows form a distinct correlated stratigraphic package which were erupted immediately prior to the large regional volcanic hiatus recorded by the coal-bearing Prestfjall Formation of the FIBG (Jolley and Whitham 2004; Passey and Jolley 2008). This hiatus was also followed by a very distinct change in facies from large classic tabular flows to the compound braided, olivine cumulative, lava flow fields of the Malinstindur Formation signalling a significant change in the flow rate and periodicity of lava flow events between the two formations (Passey and Bell 2007; Passey and Jolley 2008; Jolley et al. 2012).

Discussion

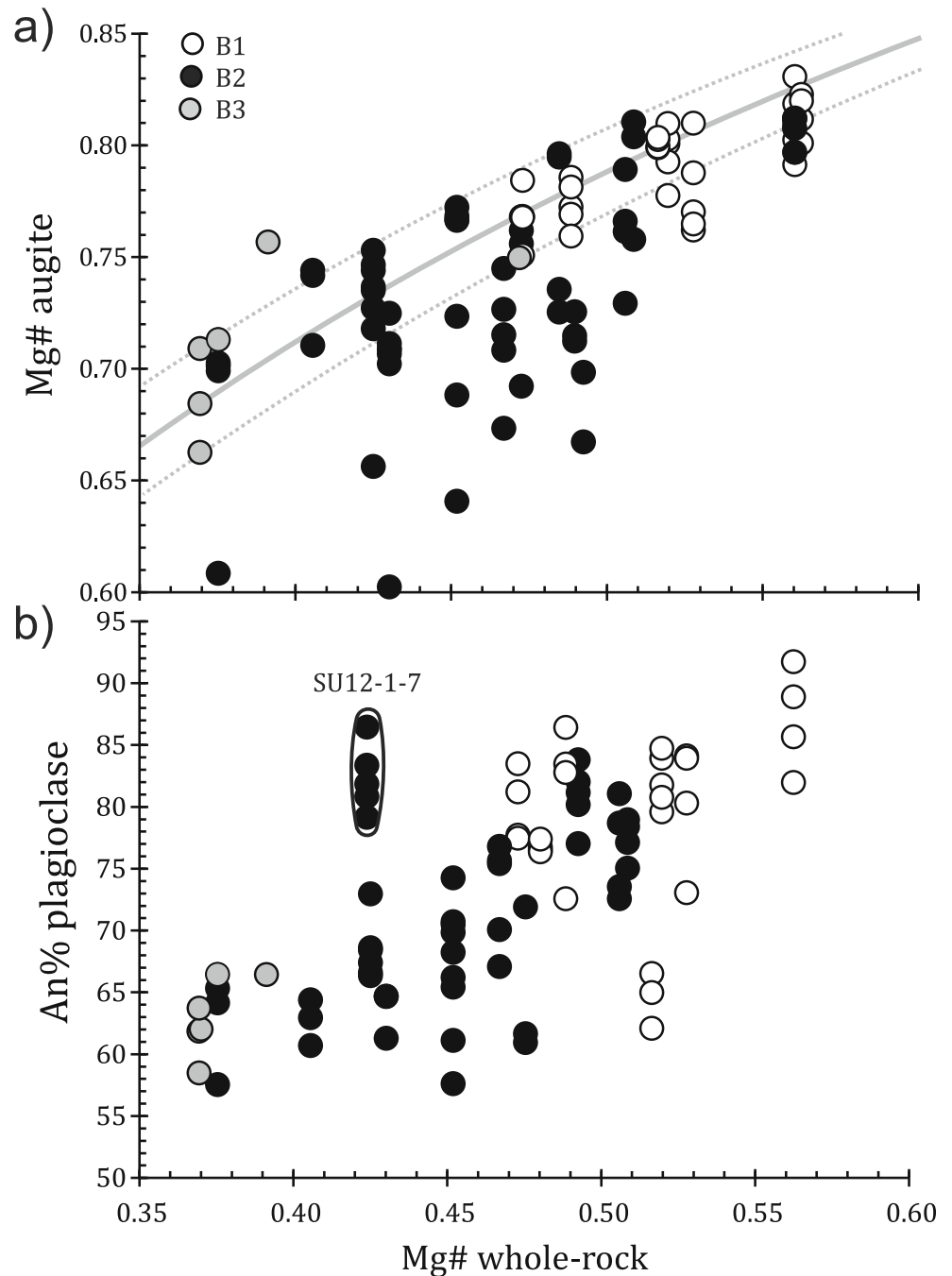
Crustal plumbing system dynamics

Petrography of the Beinivörð Formation lava flows suggests plagioclase feldspar and augite were the main crystallizing

phases. However, since all analysed samples contain < 7.8 wt% MgO, olivine crystallization is also likely to have occurred requiring significant volumes of accumulative olivine to be present at depth. However, since the relative order of crystallization of olivine, augite and plagioclase in tholeiitic magmas is strongly pressure dependent (Villiger et al. 2004; Villiger et al. 2006; Whitaker et al. 2006; Hole 2018), and there is good evidence to suggest that some NAIP lava flows fractionated at c. 1 GPa (Thompson 1974, 1982; Hole 2018), it is informative to assess the pressure conditions under which the Beinivörð Formation lava flows initially crystallized.

Two main approaches have been used in order to assess the pressure at which the Beinivörð Formation lava flows equilibrated, one utilizing whole-rock data alone and the other utilizing the composition of phenocrysts. Herzberg (2004) showed that the molecular projection from or towards olivine onto the diopside (Di), anorthite (An) and enstatite (En) plane can be used to determine pressure of fractionation for basalt compositions that lie on the liquid + olivine + plagioclase + augite cotectic. This is because the proportion of An in the projection increases systematically with increasing pressure (Fig. 11). Assessing whether samples lie on the ternary cotectic is not a trivial problem (Hole 2018). However, in the Di-An-En projection, cotectic lava flows fall along linear trajectories that project back to the Di-An divide, the proportion of An along the divide being controlled by pressure of fractionation. For samples on the L+Ol+Pl cotectic, the crystallization vector is perpendicular to that for L+Ol+Pl+Aug.

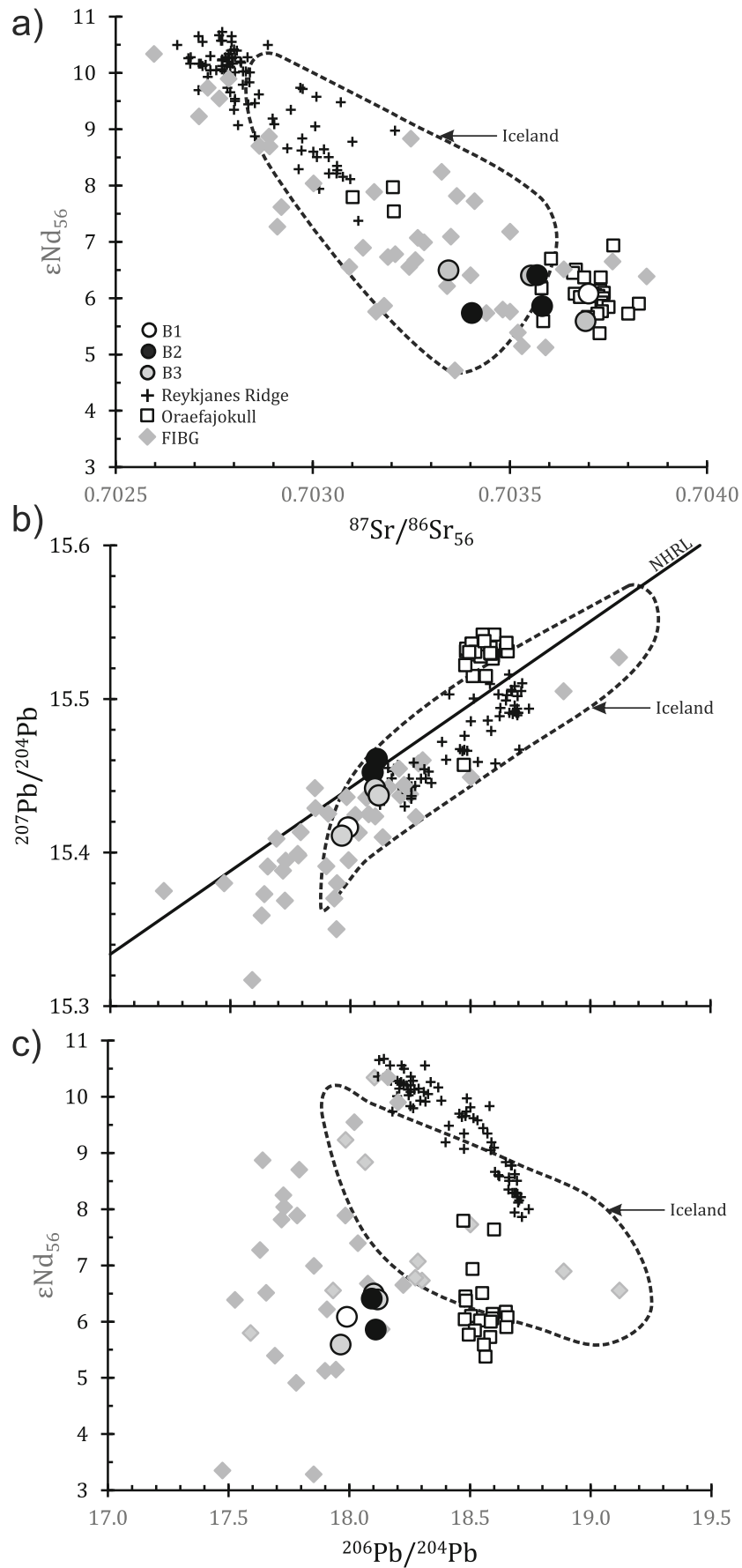
Fig. 8 (a) Augite Mg# and, (b) plagioclase An % versus whole-rock Mg#. Symbols as for Fig. 1. In (a), the grey line and two grey curves are for the equilibrium condition $kD[\text{Fe-Mg}]_{\text{Cpx-L}} = 0.27 \pm 0.03$ (Putirka 2008)



To illustrate this, data from the variable pressure crystallization experiments of Whitaker et al. (2006) are shown in Fig. 11. The starting material is I260, which is an olivine tholeiite. Since the projection is from or towards olivine, crystallization along the olivine liquidus has no effect on the position of a basalt analysis in the projection. At 1 atm (laboratory ambient pressure) for experimental compositions with olivine and plagioclase on the liquidus, the crystallization trajectory projects towards $\sim\text{An}_{75}$ with increasing temperature. Once augite joins the crystallizing assemblage, the trajectory rotates 90° and crystallization proceeds towards the En apex

along the pressure-dependent cotectics shown in Fig. 11. Also shown in Fig. 11 are experimentally determined L+Ol+Pl+

Fig. 9 (a) ϵNd_{56} versus $^{87}\text{Sr}/^{86}\text{Sr}_{56}$, (b) $^{207}\text{Pb}/^{204}\text{Pb}$ versus $^{206}\text{Pb}/^{204}\text{Pb}$ and (c) ϵNd_{56} versus $^{206}\text{Pb}/^{204}\text{Pb}$ for Beinisvörð Formation lava flows analysed in this study (subscript 56 denotes ratios corrected to 56 Ma—see Table 2). Also shown for comparison are lava flows from the Reykjanes Ridge (Murton et al. 2002), Oraefajökull (Iceland) lava flows (Torsvik et al. 2015) and selected published data for the FIBG (Gariépy et al. 1983; Søager and Holm 2009, 2011). The field for Iceland is based on data from Georoc



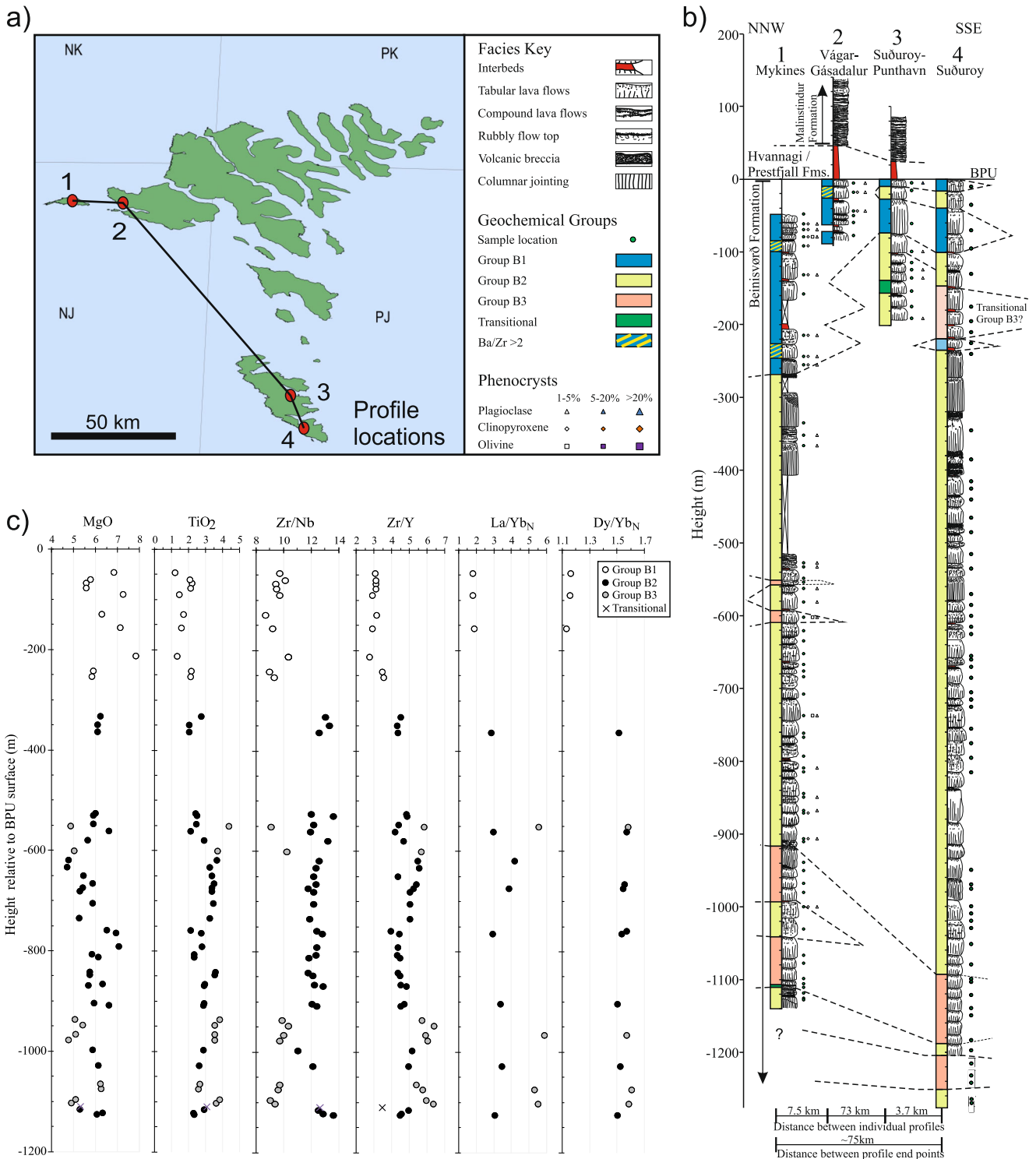


Fig. 10 **a** Overview map showing the locations of the sampled stratigraphic profiles numbered in order as presented in **b**. **b** Summary stratigraphic columns for the upper Beinisvörð Formation sample profiles with the separate geochemical groups annotated. Simplified stratigraphic tie lines are added to highlight potential correlations for illustration

purposes. **c** Stratigraphic geochemical profiles for the main Mykines (profile 1) displaying selected elements and element ratios including chondrite (Sun and McDonough 1989) normalized La/Yb_N and Dy/Yb_N ratios

Aug cotectic compositions at 0.28–0.93 GPa of Whitaker et al. (2007) which fall close to the model cotectics of Herzberg (2004) once the inherent uncertainty of ± 0.28 GPa

is accounted for (Herzberg 2004). The MgO content at which the ternary cotectic is reached for the experiments of Whitaker et al. (2007) is generally < 7.0 wt% MgO and consequently in

Fig. 11 a Molecular projection from or towards olivine (Ol) onto the plane; diopside-anorthite-enstatite (Di-An-En) using the projection coordinates given in Herzberg (2004). Isobars for crystallization along the liquid + olivine + plagioclase + augite cotectic are from Herzberg (2004). For comparison, residual liquids from the crystallization of olivine + plagioclase + augite at 0.28, 0.43, 0.68 and 0.93 GPa are shown and are taken from the melting experiments of Wilkinson et al. (2017). The thick black dashed curve is the thermal divide between olivine gabbro and norite after Herzberg (2004). **b** Expanded version of **a** showing the distribution of Beinisvørð Formation lava flows analysed for this study

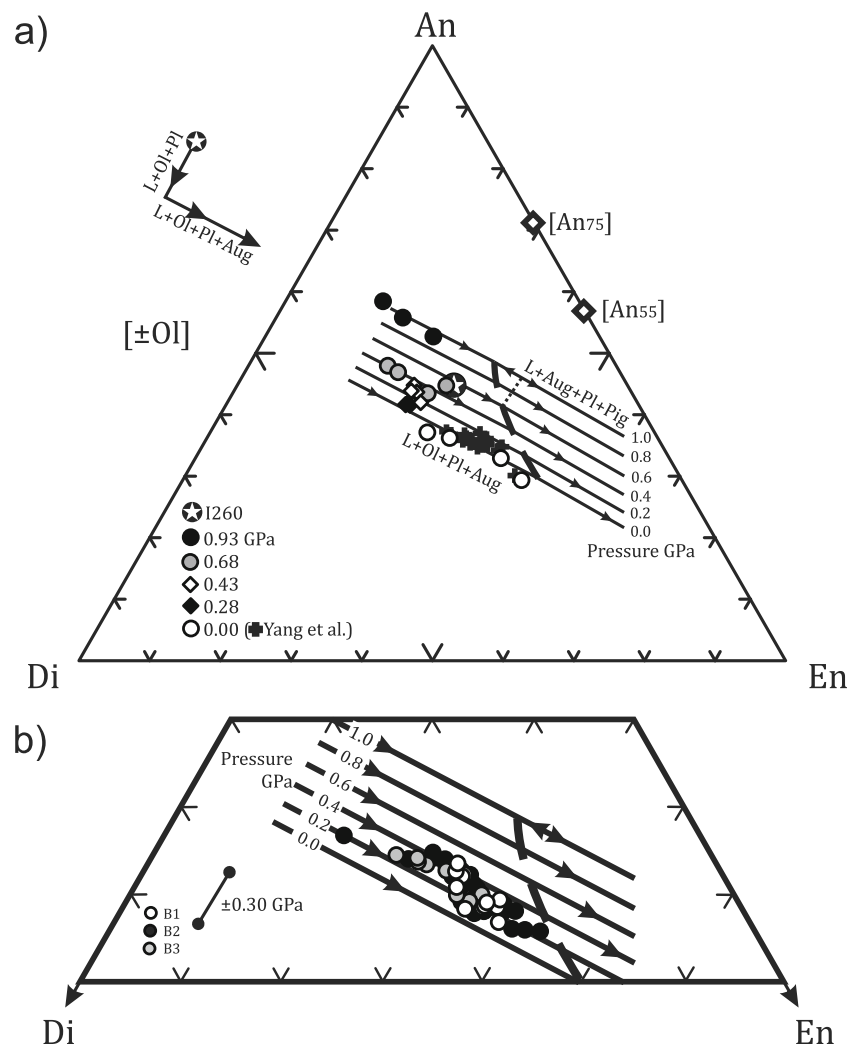


Fig. 11 b data are shown for Beinisvørð Formation lava flows with < 7.0 wt% MgO and data fall along ternary cotectic for 0.30 ± 0.10 GPa and all data falls at < 0.5 GPa. It is, therefore, concluded that the Beinisvørð Formation lava flows crystallized at ≤ 0.4 GPa and that no systematic difference in the pressure of crystallization is evident between the different groups.

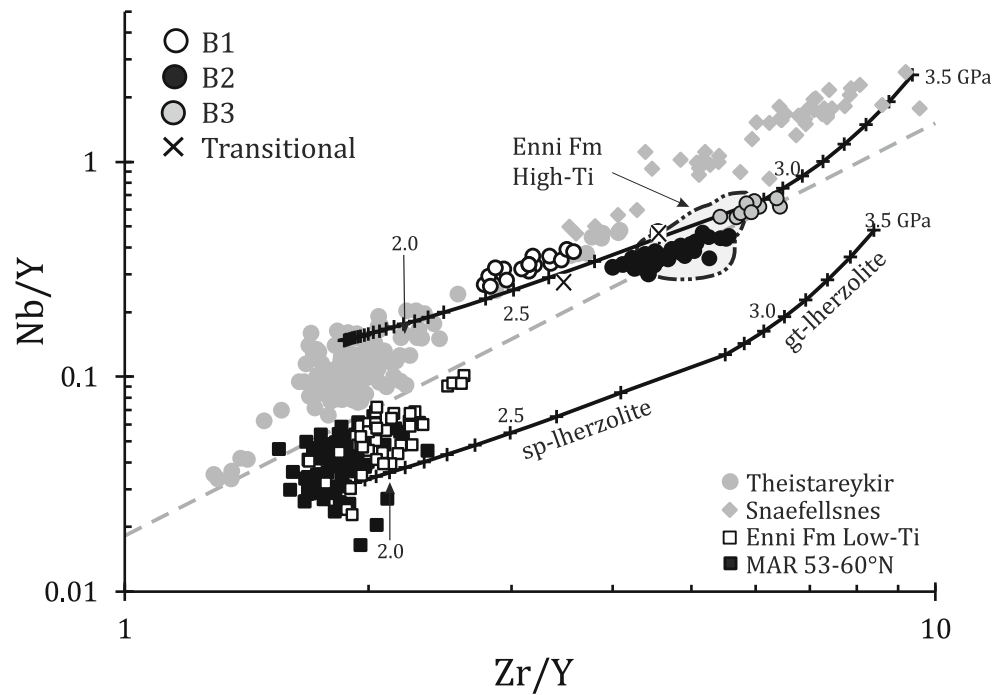
Putirka (2008) provides methods of calculating pressure of fractionation from both augite compositions and augite-whole-rock equilibria. Tests for equilibrium between clinopyroxene and a nominal coexisting liquid can be made by comparing observed and predicted values for Fe-Mg exchange ($K_{D(Fe-Mg)}^{cpx-liquid}$) which should be 0.27 ± 0.03 . Five Beinisvørð Formation lava flows and component augite phenocrysts satisfy this condition (see Online Resource 4) and provide pressure estimates of 0.50 ± 0.20 GPa using both equations [30] and [31] of Putirka (2008), assuming anhydrous crystallization conditions. Increasing water content to 0.5 wt% in the whole rock causes a small increase in pressure estimate to 0.53 ± 0.20 GPa. The model by Neave and Putirka

(2017) for clinopyroxene-rock equilibrium gives 0.39 ± 0.17 GPa for the same samples. An alternate pressure estimate using augite compositions alone utilizing equations [32a] and [32b] of Putirka (2008) yields estimates of 0.34 ± 0.17 and 0.29 ± 0.14 GPa respectively.

The combined pressure estimates obtained using the method of Herzberg (2004) and those for augite and augite-liquid equilibria are thus consistent and suggest crystallization at ≤ 0.4 GPa. At this pressure, for a tholeiitic magma under anhydrous conditions, the order of crystallization would be $L+Ol \rightarrow L+Ol+Pl \rightarrow L+Ol+Pl+Aug$. Assuming an average lithospheric density of 3.0 g/cm^3 , such a fractionation history would require a magma chamber to have been present at ≤ 12 -km depth.

For crystallization at ≤ 0.4 GPa and for any reasonable mantle potential temperature (T_P), and even for ambient T_P ($1350 \text{ }^\circ\text{C}$; Herzberg and Asimow 2015), substantial olivine crystallization must have occurred prior to the eruption of even the most MgO-rich Beinisvørð Formation lava flows. Primary magma compositions derived from PRIMELT3

Fig. 12 Nb/Y versus Zr/Y for Beinisvörð Formation lava flows (this study), Enni Formation Low-Ti and High-Ti lava flows (Millett et al. 2017; Søager and Holm 2011), Reykjanes Ridge MORB 53–60°N (Murton et al. 2002), Theistareykir (Iceland) rift zone lava flows and ‘enriched’ Icelandic lava flows from Snaefellsnes (after Fitton et al. 1997). Curves are for accumulated fractional melting of an ‘Icelandic’ and MORB source asthenosphere, the compositions of which are illustrated in Fig. 8. The dashed grey line is the dividing line between Icelandic (above the line) and MORB source-derived lava flows of Fitton et al. (1997)



modelling of Enni Formation FIBG lava flows were presented by Hole and Millett et al. (2016), and have been used to test the crystallization sequence of FIBG magmas using the Petrolog3 forward crystallization model (Danyushevsky and Plechov 2011). No clear evidence for melting of anything other than mantle peridotite is observed on the Faroe Islands and therefore, for the purposes of this discussion, a mantle peridotite mantle source is assumed.

A primary magma formed at $T_p = 1450$ °C would have ~ 15.5 wt% MgO and for crystallization at 0.4 GPa and for an oxidation state of QFM-1, plagioclase would join the crystallizing assemblage at ~9.3 wt% MgO (~15% crystallization) followed by augite at 9.0 wt% MgO (~22% crystallization). For crystallization at 0 GPa, the L+Ol+Pl crystallization interval covers a large range of MgO with augite joining the assemblage at 7.7 wt% MgO (~28% crystallization). Therefore, >15% crystallization of olivine ± plagioclase was likely required to generate the most MgO-rich Beinisvörð Formation lava flows, but the products of such crystallization are not seen at the surface and are anticipated to be linked to substantial olivine cumulates at depth. The forward Petrolog model assumes that the magmas were anhydrous. Whilst this might be an oversimplification, there is no a priori evidence that these magmas contained any water. This is similar to the situation for West Greenland where it has been demonstrated that magmas were dry (Jamtveit et al. 2001). However, we acknowledge that elsewhere in the NAIP (e.g. Iceland, East Greenland; Nichols et al. 2002; Jamtveit et al. 2001), H₂O contents of up to 300 ppm in the mantle are implied from undegassed pillow lavas and H₂O in olivine. The main effect on the Faroe Islands magmas would be an increase in the

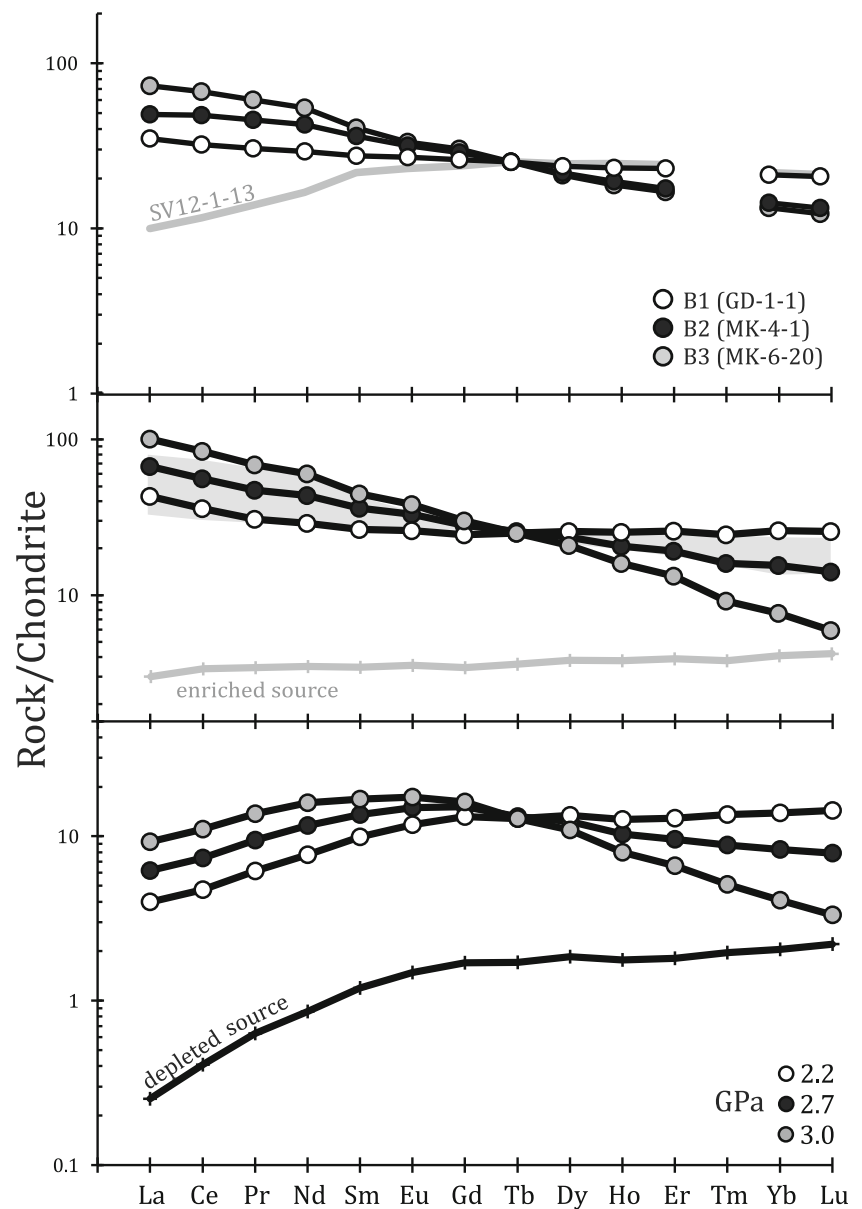
initial pressure of melting for a given TP, or suppression of the solidus to a lower TP for a given pressure (Sarafian et al. 2017). The effects of water on the petrogenesis of NAIP magmas are considered in detail in Hole and Natland (2019).

The first lava flows erupted in the overlying Malinstindur Formation are basalt and picrites with up to 23 wt% MgO (Waagstein and Hald 1984; Jolley et al. 2012). However, these do not represent liquid compositions, but instead represent olivine cumulates with minor augite (Jolley et al. 2012). These olivine cumulates have no representatives within the Beinisvörð Formation.

Mantle sources and melting

The majority of the intra-group major and trace element variations for Beinisvörð Formation lava flows can be attributed to fractional crystallization of Ol+Pl+Aug at ≤0.4 GPa. The lack of isotopic variability in the analysed samples also implies that crustal contamination was limited and that no major differences in isotopic source characteristics are evident. Consequently, variability in trace element abundances between the different groups of lava flows must be largely under the control of variations in melting and/or source composition. Hole (2018) and Hole and Natland (2019) address the possible role of pyroxenite in the source of NAIP magmas, including those of the Faroe Islands. Neither the chemistry of component olivines nor the whole-rock compositions indicate a significant pyroxenitic component in the source of basalts. Although a contribution from pyroxenite cannot be completely excluded, we consider that any substantial contribution from pyroxenite to the source of Faroe Islands lavas is

Fig. 13 (a) Observed REE patterns for Group B1–B3 Beinissvørð Formation lava flows and LREE-depleted Enni Formation Low-Ti lava SV12-1-13 (Millett et al. 2017). Model REE patterns for accumulated fractional melts formed at 2.2, 2.7 and 3.0 GPa from; (b) the proposed Beinissvørð Formation source, and (c) a ‘depleted’ Enni Formation source. Melting was assumed to commence at 3.3 GPa with garnet on the peridotite solidus at ≥ 2.7 GPa. Partition coefficients are those of McKenzie and O’Nions (1991). These patterns are normalized to $[Tb]_N = 25$ to take into account differences in absolute REE abundances that result from fractional crystallization



unlikely and therefore the following discussion is based on the assumption of a peridotite mantle source.

Fitton et al. (1997) proposed that Zr/Y and Nb/Y can be used to characterize the source from which NAIP magmas were derived and that lava flows from Iceland rift zones (Theistareykir and the Reykjanes Peninsula) have a higher Nb/Y for a given Zr/Y than lava flows derived from MORB source asthenosphere. Fitton et al. (1997) argued that this Nb enrichment was a feature specific to the Icelandic mantle. The linkage between Nb enrichment and Icelandic or ‘Plume’ sources has been questioned (Stracke et al. 2003); however, it remains a clear and regionally important variation in NAIP magmas which can be clearly linked to differences both in mantle sources and in degree and depth of melting. Both Zr/Y and Nb/Y increase with decreasing extent of melting of the

same source (Fig. 12). Data for the Enni Formation Low-Ti (low TiO_2) lava flows form a field that overlaps with MORB suggesting derivation from a MORB-like asthenosphere source, which is consistent with their LREE-depleted profiles (Fig. 6) and with the models of Søger and Holm (2011) and Millett et al. (2017). In addition, these lava flows have isotopic compositions which are consistent with derivation from the purported North Atlantic End Member (NAEM) of Ellam and Stuart (2000).

By contrast, all Beinissvørð Formation lava flows have Zr , Nb and Y distributions that are similar to those for Enni Formation High-Ti lava flows (Søger and Holm 2011; Millett et al. 2017), requiring significantly smaller extents of melting. Groups B2 and B3 overlap with the Enni Formation High-Ti lava flows in Fig. 12; however, group B1 clearly

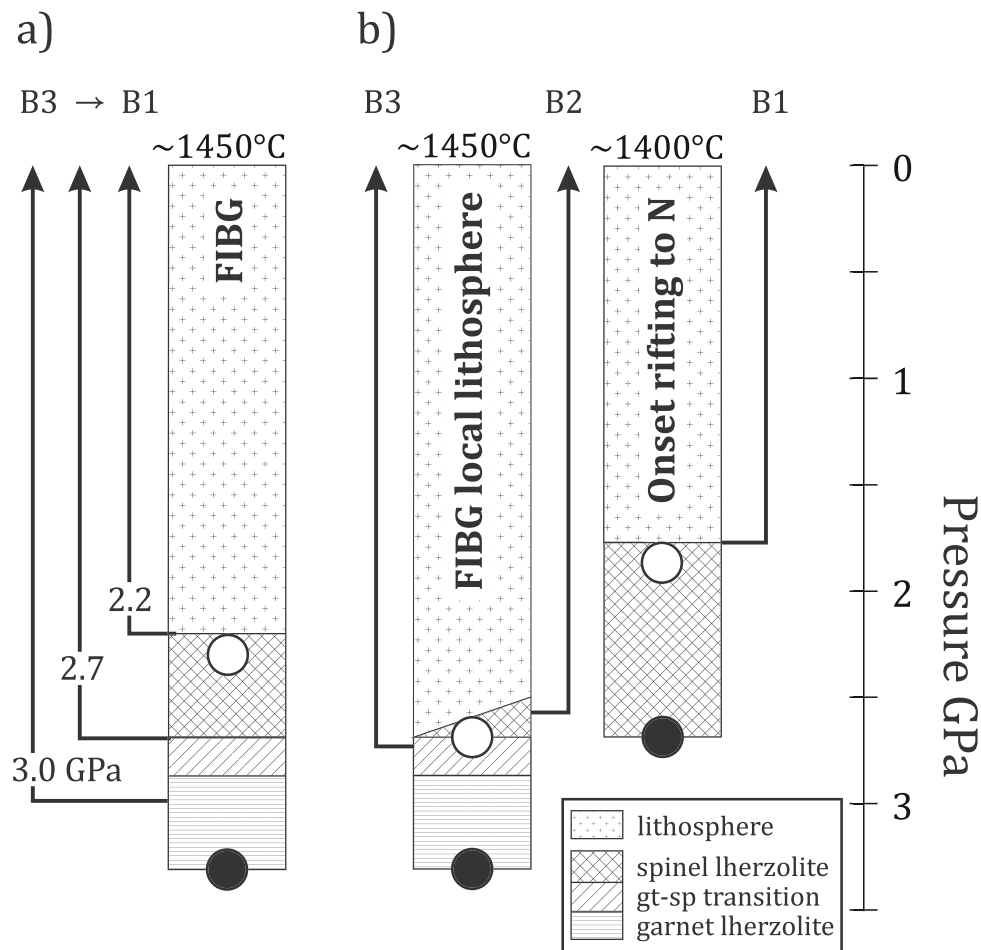


Fig. 14 Schematic 1D melting columns illustrating possible sources of the REE and incompatible trace element variability in Beinisvörð Formation lava flows after Hole and Millett et al. (2016). (a) Melting column for $\sim 1450^\circ\text{C}$ with P_i in the garnet stability field of the mantle and $P_f = 2.0$ GPa. The numbered arrows (3.0 GPa etc.) refer to the REE profiles shown in Fig. 13(b) and groups B1–B3. In this case, all lava flows were derived from the same melting regime but at different depths. Panel (b) highlights the scenario where groups B2 and B3 may be derived from similar melting conditions as in (a) but with a thicker lithosphere, whereas

Beinisvörð Formation B1 lava flows cannot be generated under the same lithospheric cap and therefore require an overall shallowing of melting caused by decreasing temperature under thinned lithosphere to the north of the Faroe Islands. In this scenario, as temperature reduces to form B1 magmas, melting would cease for B2 and B3. The garnet-spinel transition is from Robinson and Wood (1998) and the precise temperature for each melting column will depend on the peridotite solidus used as discussed in Hole and Natland (2019)

represents a separate group representing larger degrees of partial melting consistent with their weakly LREE-enriched profiles ($[\text{La}/\text{Yb}]_N \sim 1.7\text{--}2.4$). Even with the clear evidence for increased melt fraction relative to groups B2 and B3 (assuming a similar mantle source), group B1 lava flows are quite unlike the LREE-depleted nature of the Enni formation Low-Ti lava flows ($[\text{La}/\text{Yb}]_N 0.32\text{--}0.90$; Søager and Holm 2011; Millett et al. 2017). Whilst crustal contamination is known to increase La/Yb_N in NAIP lava flows (Hole et al. 2015), it also causes a concomitant increase in La/Nb , Th/Nb and Ba/Nb and these features are most evident in lava flows with negative ϵ_{Nd} . None of the Beinisvörð Formation lava flows have isotopic or trace element characteristics that suggest LREE enrichment is solely caused by crustal contamination and their LREE-enriched character must, therefore, be inherited from their mantle source.

Using mineral-melt partition coefficients for the REE from McKenzie and O’Nions (1991, 1995) and for Zr, Y and Nb from Pertermann et al. (2004), model trace element compositions are produced for melts generated from (i) a LREE-depleted MORB-like source with low Nb/Y and (ii) a source with a near-flat REE pattern and higher Nb/Y than MORB consistent with an ‘Icelandic-type’ source (Fig. 12). The model calculates accumulated fractional melts formed at 1% melt increments based on a melt productivity for peridotite of $10\% \text{ GPa}^{-1}$ (Hole and Natland 2019). The initial pressure of melting (P_i) is 3.3 GPa, which is equivalent to a T_p of $\sim 1450^\circ\text{C}$ depending on the chosen peridotite solidus (Herzberg and Asimow 2015; Hole and Millett 2016; Hole and Natland 2019) and melts that separated from the mantle at 3.0, 2.7 and 2.2 GPa pressure have been modelled. These pressures were chosen to span the garnet-spinel transition in the upper

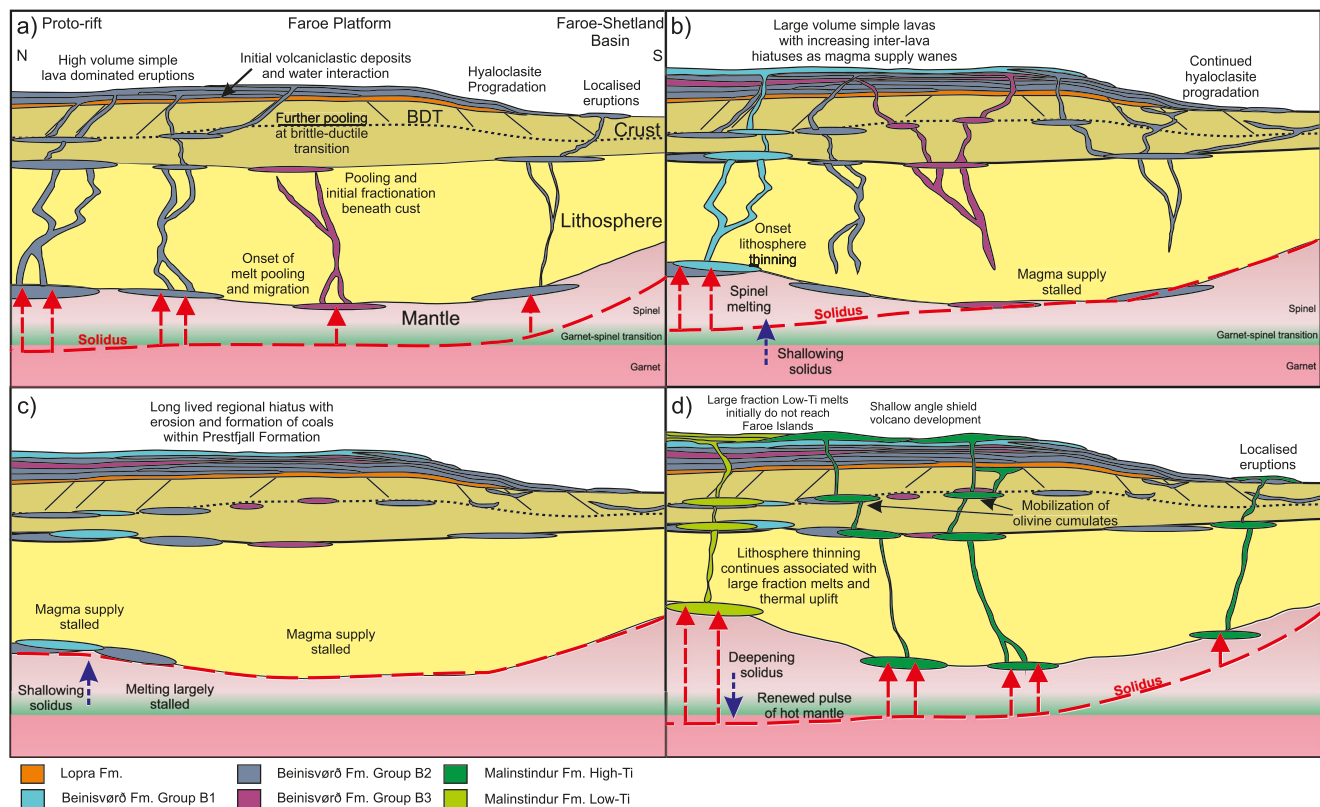


Fig. 15 Schematic evolution model highlighting the potential temporal evolution of mantle melting during the Beinisvørð Formation and early Malinstindur Formation. (a) Lopra and main phase Beinisvørð Formation development during period of elevated mantle temperature pre-breakup. (b) Onset rifting to the north of the Faroe Islands platform concomitant with a reduction in mantle temperature. (c) Regional volcanic hiatus and

deposition of Prestfjall Formation linked to continued reduction in mantle temperature. (d) Resumption of volcanism associated with renewed pulse of higher mantle temperatures leading to the eruption of the early Malinstindur Formation. Continued rifting and associated large fraction mantle melting eventually overrun the Faroe Platform likely aided by rift related uplift

mantle (Robinson and Wood 1998). Figure 13 shows that melting of a LREE-depleted source cannot produce the observed REE patterns for any of the Beinisvørð Formation lava flows. Indeed, for melting of a LREE-depleted source in the garnet-spinel transition, REE patterns show a characteristic convex upwards pattern which is common in other areas of the NAIP (e.g. British Palaeocene; Thompson 1982; Kerr et al. 1999; Hole et al. 2015), but not within the studied interval of the FIBG.

Melting of a source with a near-flat REE profile is capable of producing the observed REE patterns for Beinisvørð Formation lava flows, with the lower TiO_2 B1 lava flows ($[\text{La}/\text{Yb}]_N \sim 2$ and Dy/Yb_N c. 1.1–1.2) being generated dominantly in the presence of spinel whereas groups B2 and B3 ($[\text{La}/\text{Yb}]_N > 2.9 < 6$ and Dy/Yb_N c. 1.5–1.6) indicate a greater presence of garnet, most likely within the garnet-spinel transition of the upper mantle. The results of the same calculations for Nb/Y and Zr/Y are shown in Fig. 12, a striking feature of which is the close correspondence of the data arrays for lava flows of groups B1 to B3 with the model melting trajectory. Geochemical variations seen in the Beinisvørð Formation lava flows can, therefore, be reproduced via variable extents of

melting over different pressure melting intervals of the same mantle source.

Mantle peridotite partially melts at low melt fractions to produce melt droplets that are efficiently removed from the residue by buoyancy-driven draining. During decompression melting, the melt droplets mix to produce an ‘aggregate’ or accumulated fractional melt (AFM). In nature, mantle peridotite will melt progressively during decompression along an adiabatic P–T path, generating accumulated fractional melts that represent the weighted sum of all the melt droplets to the pressure of magma separation. The final melting pressure (P_f) represents the pressure at which the last drop of melt was produced, and this is often used as a proxy for the asthenosphere-lithosphere boundary (e.g. Hole and Millett 2016; Matzen et al. 2017; Hole and Natland 2019), and Hole and Millett et al. (2016) estimated $P_f \sim 2.0$ GPa for the shallowest melts in the upper FIBG.

It is possible that integration of all melt droplets from all pressures in the melt column is not totally efficient. For melt droplets formed closest to the surface, opportunities exist for them to avoid mixing with other increments of fractional melt (particularly those generated at higher pressure) and to erupt

as primary magmas (Herzberg et al. 2007). For example, Matthews et al. (2016) argue that in Iceland, shallow cool melts are produced from the same melting regime as deeper hotter melts and that fractional mantle melts are not completely homogenized before leaving the mantle. A similar conclusion is reached by MacLennan et al. (2003), based on trace element and olivine melt inclusion variability within an individual lava flow in northern Iceland. This is illustrated in Fig. 14 such that Beinisdvörð Formation B3 lava flows, which exhibit the greatest LREE enrichment, are derived from the deepest part of the melting column within the garnet-spinel transition in the upper mantle. Beinisdvörð Formation B1 lava flows are instead consistent with derivation dominantly from within the spinel stability field of the upper mantle whereas B2 lava flows are intermediate between these two extremes. In relation to the Beinisdvörð Formation geological setting, such a steady-state model offers no explanation for the clear stratigraphic progression of melt groups, the reduction in eruption frequency concomitant to group B1 or the subsequent long-lived Prestfjall volcanic hiatus.

Another mechanism for reducing the role of garnet during melting is to reduce the temperature of the mantle. In this case, the base of the melting column, i.e. the initial pressure of melting (P_i) would be moved to lower pressure by a decrease in temperature and towards the spinel-only stability field of the mantle. Such cooling would also be expected to cause an overall reduction in the melt fraction should the thickness of lithosphere remain constant during this interval of magmatism. For groups B2 and B3, this would give a viable explanation for stalling melt generation as the melt fractions would become too small to enable continued migration. However, for group B1, for a similar lithosphere thickness (e.g. pressure of final melting P_f), the melt fraction would also be expected to decrease, something that is not seen. Thus, in order for group B1 lavas to be produced as the result of a reduction in mantle temperature, they would also need to be generated in an area of thinner lithosphere in order to maintain a similar melt fraction as seen for the 2.2-GPa extraction model in Fig. 13. Such a model is presented schematically in Fig. 14 and would result in the same weakly LREE-enriched flat HREE pattern for B1 as modelled in Fig. 13. Whereas REE profiles are useful in determining differences between garnet- and spinel-dominated melting, REE cannot resolve variable extents of melting in the spinel field alone effectively. Melting models that are capable of resolving melt fraction from major element compositions (e.g. PRIMELT3) are not effective for cotectic liquids like those of the Beinisdvörð Formation. Therefore, constraining the melt fraction independently remains challenging.

Regional implications

Previous studies focused on the FIBG have revealed a close correlation between the FIBG and the East Greenland flood

basalt lava flow sequences (Larsen et al. 1999; Søager and Holm 2009; Millett et al. 2017), confirming that the FIBG sequence is representative of processes on both sides of the eventual continental rupture. Within the latter stages of the FIBG, there is a general trend of decreasing melt fractions within the High-Ti lava flow groups which has been linked to a similar progression on East Greenland that is interpreted as relating to a progressive reduction in mantle temperatures (Tegner et al. 1998; Søager and Holm 2009; Millett et al. 2017). During the same time interval, within the upper Malinstindur and Enni formations, depleted Low-Ti large fraction melts produced beneath rifted and thinned lithosphere between the Faroe Islands and East Greenland flowed outward from the developing rift zone across both the Faroe Islands and East Greenland for the first time in this area. The upper FIBG and East Greenland successions highlight the important point that melts produced beneath significantly different lithospheric caps occur coevally within interlayered lava sequences across wide geographical areas. This demonstrates clearly that the lava flows do not come exclusively from localized melting and that potentially significant lateral migration either through the crustal plumbing system or via long distance surface flow forms an important element of the NAIP evolution (Millett et al. 2017).

Lateral migration of melts has also been well documented in the Faroe Shetland Basin and Hebrides areas to the south (Hole et al. 2015; Schofield et al. 2017). In the Faroe-Shetland Basin, it has been proposed that dynamic topography, evidenced from seismically imaged incision envelopes within the Faroe-Shetland Basin, resulted from the convective spreading of buoyant hotter than ambient mantle beneath the lithosphere, a process attributed by several authors to pulsing of the proto-Iceland plume (Shaw-Champion et al. 2008; Saunders et al. 2007; Jones et al. 2019). To the east of the Faroe Islands in the NE Faroe-Shetland Basin, Millett et al. (2015) provided the first stratigraphically constrained petrological evidence for a linkage between dynamic changes in mantle melting and relative uplift and subsidence within the Faroe-Shetland Basin at the 217/15-1Z borehole. In this case, large fraction MORB-like melts associated with early rifting in the Møre Basin segment of the NAIP (Gernigon et al. 2019) stopped erupting in association with a volcanic hiatus that was accompanied by several hundred meters of subsidence. Volcanism resumed in the form of hydro-volcanic hyaloclastites, with an accompanying change to High-Ti locally sourced magmatism. This succession again demonstrates that melts formed under thinned lithosphere to the north within the proto-rift zone migrated southwards across an area where the local lithospheric thickness enabled only small fraction melts to be produced, e.g. High-Ti LREE-enriched melts similar to group B2 of the current study (Millett et al. 2016; Walker et al. 2020).

Within this study, we have presented the first stratigraphically constrained petrological evidence for a significant change in mantle melting during the final eruptive stages of the pre-breakup FIBG. The change in mantle melting whereby group B2 and B3 mantle melts cease to erupt and are replaced by the spinel-dominated mantle melts of B1 occurs precisely at a stratigraphically critical point in the development of the FIBG. The transition is accompanied by a clear slowing down of the eruption rate (Larsen et al. 1999; Jolley et al. 2012) and immediately precedes a long-lived volcanic hiatus during which time magmatism on the Faroe Islands and East Greenland stopped for several tens of thousands of years. As previously discussed, the two most plausible petrological options for this change in mantle melting represent (1) a transition from a well-mixed accumulative melt column to a period with poorly mixed melts and the eruption of only spinel-dominated melts, or (2) a reduction in mantle temperature causing a shallowing of the solidus to dominantly within the spinel mantle stability field. A transient change in the degree of melt column mixing fails to offer any explanation for the reduction in eruption rate or the subsequent hiatus. Therefore, we propose that a transient reduction in mantle temperature, promoting the shallowing of initial melting and eventually resulting in a temporary cessation of melting, gives a simple and intuitive explanation for the stratigraphic development of the latest Beinisvørð Formation.

REE evidence for variations in melting extent complicate this simple picture, with the B1 spinel-dominated melts indicating larger melt fractions for a given mantle source than the more garnet-influenced B2 and B3 melts. Substantial variations in lithospheric structure and thickness along the NE Atlantic margin are inherited from the long and complex tectonic history with a number of recent studies invoking complex lithospheric structure within the pre-breakup area between the Faroe Islands and East Greenland (e.g. Millett et al. 2017; Foulger et al. 2019; Gernigon et al. 2019). Therefore, it is possible that group B1 lava flows reveal evidence for the early onset of rifting and associated lithospheric thinning to the north or northwest of the Faroe Islands. In this scenario, the pre-breakup to syn-breakup transition would occur during the latter stages of the Beinisvørð Formation, earlier than previously identified.

The Prestfjall volcanic hiatus was ended with the eruption of the partly explosive Hvannhagi Formation eruptions followed by the early olivine accumulative compound lava flows of the Malinstindur Formation. The early Malinstindur successions are interpreted to form locally erupted shallow angle shield volcanoes (Noe-Nygaard, 1968; Passey and Bell 2007; Passey and Jolley 2008). It seems plausible therefore that the build-up of local shield volcanoes would have formed an effective topographic barrier to coeval, increasingly large fraction melts erupted in the developing rift zone to the north. This would explain the lack of Low-Ti large melt

fraction rift-related lava flows in the early stratigraphic sequence of the Malinstindur Formation. However, as magmatism to the north increased with continued rifting and the eruption of increasingly large volumes of Low-Ti MORB-like lava flows, eventually the local topography was overrun leading to the mixed Low and High-Ti lava flow sequences of the upper Malinstindur and Enni formations (Millett et al. 2017). Figure 15 displays a schematic evolution diagram highlighting the scenario whereby a transient reduction in mantle temperature concomitant with early onset rifting can explain the observations surrounding the pre- to syn-breakup transition of the FIBG.

The resumption of volcanism after the hiatus signals a return to mantle temperatures capable of causing renewed mantle melting, penultimately leading to the rapid eruption of over 2 km of extrusive lava flows dominated by the Malinstindur and Enni formations over the following c. 300 thousand years (Larsen and Tegner 2006). During this phase of high tempo eruptions linked to elevated mantle temperatures (Søager and Holm 2011; Millett et al. 2017), temperatures appear to have eventually begun to reduce again during the latter stages of the preserved FIBG and correlative sections on East Greenland (Tegner et al. 1998; Millett et al. 2017). Therefore, including the results of the current study, at least two large-scale transient pulses of cooler mantle temperature set against a backdrop of elevated temperatures are evidenced within the Faroe Islands stratigraphy supporting an important role for dynamic temperature fluctuations in the evolution of the NAIP.

Conclusions

This study presents an extensive new suite of high-quality geochemical analyses for stratigraphically constrained lava flows spanning over 1 km of stratigraphy focused on the final stages of the pre-breakup Beinisvørð Formation of the FIBG. The following conclusions can be drawn from this study:

1. Based on incompatible trace elements including Zr/Y/Nb and the REE, three clearly separate magma groups are defined within the upper Beinisvørð Formation.
2. Sr, Nd and Pb isotopic signatures indicate minimal interaction with continental crust and support a common mantle source for the separate groups.
3. REE element signatures suggest that High-Ti groups B2 and B3 were derived from small fraction mantle melting of peridotite in the presence of garnet and spinel, whereas group B1 lower Ti lava flows were sourced from slightly larger melt fractions, dominantly in the spinel mantle stability field, and importantly occur only at the very top of the stratigraphic sequence.
4. This change in melting was accompanied by a reduction in eruption rate evidenced by increasing thicknesses and

durations of inter-lava sediments leading up to a regional volcanic hiatus during which time the coal-bearing Prestfjall Formation was developed.

These observations support a scenario in which a regional reduction in mantle temperature occurred concomitant with the early onset of rifting and lithospheric thinning to the north or northwest of the Faroe Islands during the latest Beinisvørð Formation time. In this scenario, the pre-breakup to syn-breakup transition between the Faroe Islands and East Greenland would occur prior to the regional hiatus and earlier than previously identified in this region.

This study reveals the first onshore petrological evidence for a reduction in mantle temperature leading to the regional volcanic hiatus associated with the pre-breakup to syn-breakup transition in the NAIP. The volcanic hiatus was ended by explosive eruptions of the Hvannahagi Formation followed by olivine cumulate-bearing compound lava flows of the Malinstindur Formation signalling a return of elevated mantle temperatures. In conjunction with previous evidence for waning mantle temperatures later in the development of the FIBG and East Greenland, this study proposes repeated transient mantle temperature fluctuations during the main phase of NAIP volcanism. This implies that both dynamic temperature fluctuations and rifting history are tightly interwoven and that any generalized models for the NAIP evolution must take both into account.

Acknowledgments The authors would like to thank Romica Øster at Jarðfeingi for assistance with sample shipping from the Faroe Islands, John Still and Walter Ritchie at the University of Aberdeen for assistance with probe work and slide preparation and Thomas Varming for assistance with fieldwork. John Watson and Sam Malley from the OU are thanked for geochemical analyses. Simon Matthews and two anonymous reviewers gave detailed and constructive reviews which substantially improved the manuscript and Nicole Métrich is kindly thanked for editorial handling.

Open Access This article is licensed under a Creative Commons Attribution 4.0 International License, which permits use, sharing, adaptation, distribution and reproduction in any medium or format, as long as you give appropriate credit to the original author(s) and the source, provide a link to the Creative Commons licence, and indicate if changes were made. The images or other third party material in this article are included in the article's Creative Commons licence, unless indicated otherwise in a credit line to the material. If material is not included in the article's Creative Commons licence and your intended use is not permitted by statutory regulation or exceeds the permitted use, you will need to obtain permission directly from the copyright holder. To view a copy of this licence, visit <http://creativecommons.org/licenses/by/4.0/>.

References

- Anderson DL (2013) The persistent mantle plume myth. *Aust J Earth Sci* 60:657–673. <https://doi.org/10.1080/08120099.2013.835283>
- Champion MES, White NJ, Jones SM, Lovell JPB (2008) Quantifying transient mantle convective uplift: an example from the Faroe-Shetland basin. *Tectonics* 27:n/a. <https://doi.org/10.1029/2007TC002106>
- Clarke DB, Beutel EK (2019) Davis Strait Paleocene picrites: products of a plume or plates? *Earth-Science Rev* 0–1. <https://doi.org/10.1016/j.earscirev.2019.01.012>
- Danyushevsky LV, Plechov P (2011) Petrolog3: integrated software for modeling crystallization processes. *Geochem Geophys Geosyst* 12:n/a. <https://doi.org/10.1029/2011GC003516>
- Ellam RM, Stuart FM (2000) The sub-lithospheric source of North Atlantic basalts: evidence for, and significance of, a common end-member. *J Petrol* 41:919–932. <https://doi.org/10.1093/petrology/41.7.919>
- Fitton JG, Saunders AD, Norry MJ, Hardarson BS, Taylor RN (1997) Thermal and chemical structure of the Iceland plume. *Earth Planet Sci Lett* 153:197–208. [https://doi.org/10.1016/S0012-821X\(97\)00170-2](https://doi.org/10.1016/S0012-821X(97)00170-2)
- Fitton JG, Saunders AD, Larsen HC, et al (1998) Volcanic rocks from the East Greenland margin at 63N: composition, petrogenesis and mantle sources. In: S. SADLHCW, Allen JR (eds) Saunders. Proceedings of the Ocean Drilling Program, Scientific Results, 152. Ocean Drilling Program, College Station, TX, 331–350, pp 331–350
- Foulger GR, Doré T, Emelous CH, Franke D, Geoffroy L, Gemigon L, Hey R, Holdsworth RE, Hole M, Höskuldsson Á, Julian B, Kuszniir N, Martinez F, McCaffrey KJW, Natland JH, Peace AL, Petersen K, Schiffer C, Stephenson R, Stoker M (2019) The Iceland microcontinent and a continental Greenland-Iceland-Faroe ridge. *Earth-Sci Rev* 102926:102926. <https://doi.org/10.1016/j.earscirev.2019.102926>
- Gariépy C, Ludden J, Brooks C (1983) Isotopic and trace element constraints on the genesis of the Faeroe lava pile. *Earth Planet Sci Lett* 63:257–272. [https://doi.org/10.1016/0012-821X\(83\)90041-9](https://doi.org/10.1016/0012-821X(83)90041-9)
- Gernigon L, Franke D, Geoffroy L, Schiffer C, Foulger GR, Stoker M (2019) Crustal fragmentation, magmatism, and the diachronous opening of the Norwegian-Greenland Sea. *Earth-Science Rev*: 102839. <https://doi.org/10.1016/j.earscirev.2019.04.011>
- Hald N, Waagstein R (1984) Lithology and chemistry of a 2-km sequence of Lower Tertiary tholeiitic lavas drilled on Suðuroy, Faeroe Islands (Lopra-1). In: Berthelsen O, Noe-Nygaard A, Rasmussen J (eds) The deep drilling project 1980–1981 in the Faeroe Islands. *Annales Societatis Scientiarum Færoensis, Tórshavn*, pp 15–38
- Hartley RA, Roberts GG, White N, Richardson C (2011) Transient convective uplift of an ancient buried landscape. *Nat Geosci* 4:562–565. <https://doi.org/10.1038/ngsci1191>
- Herzberg C (2004) Partial crystallization of mid-ocean ridge basalts in the crust and mantle. *J Petrol* 45:2389–2405. <https://doi.org/10.1093/petrology/egh040>
- Herzberg C, Asimow PD (2015) PRIMELT3 MEGA.XLSM software for primary magma calculation: peridotite primary magma MgO contents from the liquidus to the solidus. *Geochem Geophys Geosyst* 16:563–578. <https://doi.org/10.1002/2014GC005631>
- Herzberg C, Asimow PD, Amdt N et al (2007) Temperatures in ambient mantle and plumes: constraints from basalts, picrites, and komatiites. *Geochem Geophys Geosyst* 8:n/a. <https://doi.org/10.1029/2006GC001390>
- Hole MJ (2018) Mineralogical and geochemical evidence for polybaric fractional crystallization of continental flood basalts and implications for identification of peridotite and pyroxenite source lithologies. *Earth-Sci Rev* 176:51–67. <https://doi.org/10.1016/j.earscirev.2017.09.014>
- Hole MJ, Millett JM (2016) Controls of mantle potential temperature and lithospheric thickness on magmatism in the North Atlantic Igneous Province. *J Petrol* 57:417–436. <https://doi.org/10.1093/petrology/egw014>

- Hole MJ, Natland JH (2019) Magmatism in the North Atlantic Igneous Province; mantle temperatures, rifting and geodynamics. *Earth-Sci Rev*. <https://doi.org/10.1016/j.earscirev.2019.02.011>
- Hole MJ, Millett JM, Rogers NW, Jolley DW (2015) Rifting and mafic magmatism in the Hebridean basins. *J Geol Soc Lond* 172:218–236. <https://doi.org/10.1144/jgs2014-100>
- Irvine TN, Baragar WRA (1971) A guide to the chemical classification of the common volcanic rocks. *Can J Earth Sci* 8:523–548. <https://doi.org/10.1139/e71-055>
- Ishizuka O, Taylor RN, Geshi N, Mochizuki N (2017) Large-volume lateral magma transport from the Mull volcano: an insight to magma chamber processes. *Geochem Geophys Geosyst* 18:1618–1640. <https://doi.org/10.1002/2016GC006712>
- Jamtveit B, Brooker R, Brooks K, Larsen LM, Pedersen T (2001) The water content of olivines from the North Atlantic Volcanic Province. *Earth Planet Sci Lett* 186:401–415. [https://doi.org/10.1016/S0012-821X\(01\)00256-4](https://doi.org/10.1016/S0012-821X(01)00256-4)
- Jerram DA (2002) Volcanology and facies architecture of flood basalts. In: Menzies MA, Klemperer SL, Ebinger CJ, Baker J, (eds) *Volcanic Rifted Margins*. *Geol Soc Am Spec Pap*, 362: 119–132
- Jolley DW, Bell BR (2002) The evolution of the North Atlantic Igneous Province and the opening of the NE Atlantic rift. *Geol Soc Lond Spec Publ* 197:1–13. <https://doi.org/10.1144/GSL.SP.2002.197.01.01>
- Jolley DW, Whitham AG (2004) A stratigraphical and palaeoenvironmental analysis of the sub-basaltic Palaeogene sediments of East Greenland. *Pet Geosci* 10:53–60. <https://doi.org/10.1144/1354-079302-511>
- Jolley DW, Passey SR, Hole M, Millett J (2012) Large-scale magmatic pulses drive plant ecosystem dynamics. *J Geol Soc Lond* 169:703–711. <https://doi.org/10.1144/jgs2012-012>
- Jones SM, Hoggett M, Greene SE, Jones TD (2019) Large Igneous Province thermogenic greenhouse gas flux could have initiated Paleocene-Eocene thermal maximum climate change. *Nat Commun* 10:1–16
- Kerr AC, Kempton PD, Thompson RN (1995) Crustal assimilation during turbulent magma ascent (ATA); new isotopic evidence from the Mull Tertiary lava succession. *N W Scotland Contrib to Mineral Petrol* 119:142–154. <https://doi.org/10.1007/BF00307277>
- Kerr AC, Kent RW, Thomson BA, Seedhouse JK, Donaldson CH (1999) Geochemical evolution of the tertiary Mull volcano, Western Scotland. *J Petrol* 40:873–908. <https://doi.org/10.1093/ptro/40.6.873>
- Koptev A, Cloetingh S, Burov E, François T, Gerya T (2017) Long-distance impact of Iceland plume on Norway's rifted margin. *Sci Rep* 7:10408. <https://doi.org/10.1038/s41598-017-07523-y>
- Larsen HC, Saunders AD (1998) Tectonism and volcanism at the Southeast Greenland rifted margin: a record of plume impact and later continental rapture. In: *Proceedings of the Ocean Drilling Program, 152 Scientific Results*. Ocean Drilling Program, pp 503–533
- Larsen LM, Fitton JG, Fram MS (1998) Volcanic rocks of the southeast Greenland Margin in comparison with other parts of the North Atlantic tertiary igneous province. In: *Proceedings of the Ocean Drilling Program, 152 Scientific Results*. Ocean Drilling Program, pp 315–330
- Larsen RB, Tegner C (2006) Pressure conditions for the solidification of the Skaergaard intrusion: eruption of East Greenland flood basalts in less than 300,000 years. *Lithos* 92:181–197. <https://doi.org/10.1016/j.lithos.2006.03.032>
- Larsen LM, Watt WS, Watt M (1989) Geology and petrology of the Lower Tertiary plateau basalts of the Scoresby Sund region, East Greenland. *Geol Greenl Surv Bull* 157:1
- Larsen LM, Waagstein R, Pedersen AK, Storey M (1999) Trans-Atlantic correlation of the Palaeogene volcanic successions in the Faeroe Islands and East Greenland. *J Geol Soc Lond* 156:1081–1095. <https://doi.org/10.1144/gsjgs.156.6.1081>
- Larsen LM, Pedersen AK, Tegner C, Duncan RA (2014) Eocene to Miocene igneous activity in NE Greenland: northward younging of magmatism along the East Greenland margin. *J Geol Soc Lond* 171:539–553. <https://doi.org/10.1144/jgs2013-118>
- Le Maitre RW et al (2002) A classification of igneous rocks and glossary of terms: recommendations of the International Union of Geological Sciences Subcommittee on the Systematics of Igneous Rocks. Cambridge University Press, Cambridge
- Lyle P (2000) The eruption environment of multi-tiered columnar basalt lava flows. *J Geol Soc Lond* 157:715–722. <https://doi.org/10.1144/jgs.157.4.715>
- MacLennan J, McKenzie D, Hilton F et al (2003) Geochemical variability in a single flow from northern Iceland. *J Geophys Res Solid Earth* 108:ECV-4
- Matthews S, Shorttle O, MacLennan J (2016) The temperature of the Icelandic mantle from olivine-spinel aluminum exchange thermometry. *Geochem Geophys Geosyst* 17:4725–4752. <https://doi.org/10.1002/2016GC006497>
- Matzen AK, Baker MB, Beckett JR, Wood BJ (2017) The effect of liquid composition on the partitioning of Ni between olivine and silicate melt. *Contrib Mineral Petrol* 10:1318–1319. DOI. <https://doi.org/10.1007/s00410-016-1319-8>
- McKenzie D, O'Nions RK (1991) Partial melt distributions from inversion of rare earth element concentrations. *J Petrol* 32:1021–1091. <https://doi.org/10.1093/ptrology/32.5.1021>
- McKenzie D, O'Nions RK (1995) The source regions of ocean island basalts. *J Petrol* 36:133–159. <https://doi.org/10.1093/ptrology/36.1.133>
- Millett, J.M., 2014. *Geochemical stratigraphy and correlation within the Faroe Islands Basalt Group with developments in the analysis of Large Igneous Province deposits from well data* (Doctoral dissertation, University of Aberdeen)
- Millett JM, Hole MJ, Jolley DW, Schofield N, Campbell E (2016) Frontier exploration and the North Atlantic Igneous Province: new insights from a 2.6 km offshore volcanic sequence in the NE Faroe-Shetland Basin. *J Geol Soc Lond* 173:320–336. <https://doi.org/10.1144/jgs2015-069>
- Millett JM, Hole MJ, Jolley DW, Passey SR (2017) Geochemical stratigraphy and correlation within large igneous provinces: the final preserved stages of the Faroe Islands Basalt Group. *Lithos* 286–287:1–15. <https://doi.org/10.1016/j.lithos.2017.05.011>
- Morgan WJ (1971) Convection plumes in the lower mantle. *Nature* 230: 42–43
- Morrison MA (1978) The use of “immobile” trace elements to distinguish the palaeotectonic affinities of metabasalts: applications to the Palaeocene basalts of Mull and Skye, NW Scotland. *Earth Planet Sci Lett* 39:407–416
- Murton BJ, Taylor RN, Thirwall MF (2002) Plume-Ridge Interaction: a Geochemical Perspective from the Reykjanes Ridge. *J Petrol* 43: 1987–2012. <https://doi.org/10.1093/ptrology/43.11.1987>
- Neave DA, Putirka KD (2017) A new clinopyroxene-liquid barometer, and implications for magma storage pressures under Icelandic rift zones. *Am Mineral* 102:777–794. <https://doi.org/10.2138/am-2017-5968>
- Nichols ARL, Carroll MR, Höskuldsson Á (2002) Is the Iceland hot spot also wet? Evidence from the water contents of undegassed submarine and subglacial pillow basalts. *Earth Planet Sci Lett* 202:77–87. [https://doi.org/10.1016/S0012-821X\(02\)00758-6](https://doi.org/10.1016/S0012-821X(02)00758-6)
- Parnell-Turner R, White N, Henstock T, Murton B, MacLennan J, Jones SM (2014) A continuous 55-million-year record of transient mantle plume activity beneath Iceland. *Nat Geosci* 7:914–919
- Passey SR (2004) The volcanic and sedimentary evolution of the Faeroe Plateau Lava Group, Faeroe Islands and the Faeroe-Shetland Basin, NE Atlantic. Unpublished. University of Glasgow

- Passey SR (2009) Recognition of a faulted basalt lava flow sequence through the correlation of stratigraphic marker units, Skopunarfjörður, Faroe Islands. *Faroe Islands Explor Conf Proc Ann Soc Sci Færoensis*, Tórshavn 174–204
- Passey SR (2014) The habit and origin of siderite spherules in the Eocene coal-bearing Prestfjall Formation, Faroe Islands. *Int J Coal Geol* 122:76–90. <https://doi.org/10.1016/j.coal.2013.12.009>
- Passey SR, Bell BR (2007) Morphologies and emplacement mechanisms of the lava flows of the Faroe Islands Basalt Group, Faroe Islands, NE Atlantic Ocean. *Bull Volcanol* 70:139–156. <https://doi.org/10.1007/s00445-007-0125-6>
- Passey SR, Jolley DW (2008) A revised lithostratigraphic nomenclature for the Palaeogene Faroe Islands Basalt Group, NE Atlantic Ocean. *Earth Environ Sci Trans R Soc Edinburgh* 99:127–158. <https://doi.org/10.1017/S1755691009008044>
- Passey SR, Varming T (2010) Surface interpolation within a continental flood basalt province: an example from the Palaeogene Faroe Islands Basalt Group. *J Struct Geol* 32:709–723. <https://doi.org/10.1016/j.jsg.2010.04.016>
- Peace AL, Phethean JJJ, Franke D, Foulger GR, Schiffer C, Welford JK, McHone G, Rocchi S, Schnabel M, Doré AG (2019) A review of Pangaea dispersal and large igneous provinces – in search of a causative mechanism. *Earth-Science Rev* 102902:102902. <https://doi.org/10.1016/j.earscirev.2019.102902>
- Pedersen AK, Larsen LM, Pedersen GK (2017) Lithostratigraphy, geology and geochemistry of the volcanic rocks of the Vaigat Formation on Disko and Nuussuaq, Paleocene of West Greenland. *Geol Surv Denmark Greenl Bull* 39:247
- Pertermann M, Hirschmann MM, Hametner K, Günther D, Schmidt MW (2004) Experimental determination of trace element partitioning between garnet and silica-rich liquid during anhydrous partial melting of MORB-like eclogite. *Geochem Geophys Geosyst* 5. <https://doi.org/10.1029/2003GC000638>
- Petersen KD, Schiffer C, Nagel T (2018) LIP formation and protracted lower mantle upwelling induced by rifting and delamination. *Sci Rep* 8:16578. <https://doi.org/10.1038/s41598-018-34194-0>
- Putirka KD (2008) Thermometers and barometers for volcanic systems. In: Putirka KD, Tepley F (eds) *Minerals, Inclusions and Volcanic Processes, Reviews in Mineralogy and Geochemistry*, 69th edn. Mineralogical Society of America, pp 61–120
- Ramsey MH, Potts PJ, Webb PC, Watkins P, Watson JS, Coles BJ (1995) An objective assessment of analytical method precision: comparison of ICP-AES and XRF for the analysis of silicate rocks. *Chem. Geol.* 124(1-2):1–19
- Rasmussen J, Noe-Nygaard A (1970) *Geology of the Faeroe Islands (Pre-Quaternary)* [TransHenderson, G.]. Geological Survey of Denmark, Copenhagen
- Robinson JAC, Wood BJ (1998) The depth of the spinel to garnet transition at the peridotite solidus. *Earth Planet Sci Lett* 164:277–284. [https://doi.org/10.1016/S0012-821X\(98\)00213-1](https://doi.org/10.1016/S0012-821X(98)00213-1)
- Sarafian E, Gaetani GA, Hauri EH, Sarafian AR (2017) Experimental constraints on the damp peridotite solidus and oceanic mantle potential temperature. *Science* (80) 355:942–945. <https://doi.org/10.1126/science.aaj2165>
- Saunders AD, Fitton JG, Kerr AC, et al (1997) The North Atlantic Igneous Province. In: *Geophysical Monograph Series*. pp 45–93
- Saunders AD, Jones SM, Morgan LA, Pierce KL, Widdowson M, Xu YG (2007) Regional uplift associated with continental large igneous provinces: the roles of mantle plumes and the lithosphere. *Chem Geol* 241:282–318. <https://doi.org/10.1016/j.chemgeo.2007.01.017>
- Schofield N, Holford S, Millett J, Brown D, Jolley D, Passey SR, Muirhead D, Grove C, Magee C, Murray J, Hole M, Jackson CAL, Stevenson C (2017) Regional magma plumbing and emplacement mechanisms of the Faroe-Shetland Sill Complex: implications for magma transport and petroleum systems within sedimentary basins. *Basin Res* 29:41–63. <https://doi.org/10.1111/bre.12164>
- Søager N, Holm PM (2009) Extended correlation of the Paleogene Faroe Islands and East Greenland plateau basalts. *Lithos* 107:205–215. <https://doi.org/10.1016/j.lithos.2008.10.002>
- Søager N, Holm PM (2011) Changing compositions in the Iceland plume; isotopic and elemental constraints from the Paleogene Faroe flood basalts. *Chem Geol* 280:297–313. <https://doi.org/10.1016/j.chemgeo.2010.11.017>
- Sparks RSJ, Annen C, Blundy JD, Cashman KV, Rust AC, Jackson MD (2019) Formation and dynamics of magma reservoirs. *Philos Trans R Soc A* 377:20180019
- Steinberger B, Bredow E, Lebedev S, Schaeffer A, Torsvik TH (2019) Widespread volcanism in the Greenland-North Atlantic region explained by the Iceland plume. *Nat Geosci* 12:61–68
- Stoker MS, Holford SP, Hillis RR (2018) A rift-to-drift record of vertical crustal motions in the Faroe-Shetland Basin, NW European margin: establishing constraints on NE Atlantic evolution. *J Geol Soc Lond* 175:263–274
- Storey M, Duncan RA, Tegner C (2007) Timing and duration of volcanism in the North Atlantic Igneous Province: implications for geodynamics and links to the Iceland hotspot. *Chem Geol* 241: 264–281. <https://doi.org/10.1016/j.chemgeo.2007.01.016>
- Stracke A, Zindler A, Salters VJM, McKenzie D, Blichert-Toft J, Albarède F, Grönvold K (2003) Theistareykir revisited. *Geochem Geophys Geosyst* 4:1–49. <https://doi.org/10.1029/2001GC000201>
- Sun S-S, McDonough WF (1989) Chemical and isotopic systematics of oceanic basalts: implications for mantle composition and processes. *Geol Soc Lond Spec Publ* 42:313–345. <https://doi.org/10.1144/GSL.SP.1989.042.01.19>
- Svensen HH, Jerram DA, Polozov AG, Planke S, Neal CR, Augland LE, Emeleus HC (2019) Thinking about LIPs: a brief history of ideas in large igneous province research. *Tectonophysics* 760:229–251
- Tegner C, Leshner CE, Larsen LM, Watt WS (1998) Evidence from the rare-earth-element record of mantle melting for cooling of the Tertiary Iceland plume. *Nature* 395:591–594. <https://doi.org/10.1038/26956>
- Thompson RN (1974) Primary basalts and magma genesis. I. Skye, north-west Scotland. *Contrib Mineral Petrol* 45:317–341
- Thompson RN (1982) Magmatism of the British Tertiary Volcanic Province. *Scott J Geol* 18:49–107. <https://doi.org/10.1144/sjg18010049>
- Torsvik TH, Amundsen HEF, Trønnes RG, Doubrovine PV, Gaina C, Kuznir NJ, Steinberger B, Corfu F, Ashwal LD, Griffin WL, Werner SC, Jamtveit B (2015) Continental crust beneath Southeast Iceland. *Proc Natl Acad Sci* 112:E1818–E1827. <https://doi.org/10.1073/pnas.1423099112>
- Villiger S, Ulmer P, Müntener O (2006) Equilibrium and fractional crystallization experiments at 0-7 GPa; the effect of pressure on phase relations and liquid compositions of tholeiitic magmas. *J Petrol* 48: 159–184. <https://doi.org/10.1093/petrology/egl058>
- Villiger S, Ulmer P, Müntener O, Thompson AB (2004) The liquid line of descent of anhydrous, mantle-derived, tholeiitic liquids by fractional and equilibrium crystallization-an experimental study at 1-0 GPa. *J Petrol* 45:2369–2388. <https://doi.org/10.1093/petrology/egh042>
- Waaagstein R (1977) *The geology of the Faeroe plateau*. Unpubl thesis, Univ Copenhagen
- Waaagstein R (1988) Structure, composition and age of the Faeroe basalt plateau. *Geol Soc Lond Spec Publ* 39:225–238. <https://doi.org/10.1144/GSL.SP.1988.039.01.21>
- Waaagstein R (1997) *Volcanic rocks, Lopra-1/1A Faroe Islands 1996:: technical studies prepared for Dansk Olie og Naturgas A/S*. Geological Survey of Denmark and Greenland, Copenhagen
- Waaagstein R (2006) *Composite log from the Lopra-1/1A well, Faroe Islands Geol Surv Denmark Greenland Bull* 9
- Waaagstein R, Hald N (1984) Structure and petrography of a 660 m lava sequence from the Vestmanna-1 drill hole, lower and middle basalt series, Faeroe Islands. In: Berthelsen O, N-NA, Rasmussen J (eds)

- The Deep Drilling Project 1980-1981 in the Faeroe Islands, Supplementum IX. *Annales Societatis Scientiarum Færoensis*, Tórshavn, pp 39–70
- Walker F, Schofield N, Millett JM, et al (2020) Paleogene volcanic rocks in the northern Faroe–Shetland Basin and Møre Marginal High: understanding lava field stratigraphy. *Geol Soc London, Spec Publ SP495–2019–13*. <https://doi.org/10.1144/SP495-2019-13>
- Watson JS (1996) Fast, Simple Method of Powder Pellet Preparation for X-Ray Fluorescence Analysis. *X-Ray Spectrometry* 25(4):173–174
- Whitaker ML, Nekvasil H, Lindsley DH, Diffrancesco NJ (2006) The role of pressure in producing compositional diversity in intraplate basaltic magmas. *J Petrol* 48:365–393. <https://doi.org/10.1093/petrology/eg1063>
- Wilkinson CM, Ganerød M, Hendriks BWH, Eide EA (2017) Compilation and appraisal of geochronological data from the North Atlantic Igneous Province (NAIP). *Geol Soc Lond Spec Publ* 447:69–103. <https://doi.org/10.1144/SP447.10>